Agricultural and Forest Meteorology 292–293 (2020) 108127

Contents lists available at ScienceDirect

Agricultural and Forest Meteorology

journal homepage: www.elsevier.com/locate/agrformet

A modified SWAP model for soil water and heat dynamics and seed–maize growth under film mulching

Yin Zhao[a,b], Xiaomin Mao[a,b,*], Manoj K. Shukla[c]

[a] Center for Agricultural Water Research in China, China Agricultural University, No 17 Qinghua East Road, Haidian District, Beijing 100083, China
[b] Shiyanghe Experimental Station, China Agricultural University, Wuwei 733000, China
[c] Plant and Environmental Sciences, New Mexico State University, Las Cruces, NM 88003–8003, USA

ARTICLE INFO

Keywords:
Film mulching
Seed–maize growth
Soil moisture and temperature
Water balance
Modified SWAP model

ABSTRACT

Soil–Water–Atmosphere–Plant (SWAP) model fails to consider the impacts of plastic film mulching on soil moisture and heat regimes, and crop growth and yield. In this study, SWAP model was modified in the modules of precipitation interception, soil evaporation, soil temperature, and crop growth to accommodate the changes of soil moisture and soil temperature caused by film mulching and the consequent variation of crop growth. The modified SWAP model was compared with original SWAP model. Here, the original model showed the case where there was no film mulching effect under the same input conditions as the modified model. The models were calibrated and validated by a field experiment of seed–maize conducted in the Shiyang River Basin of Northwest China in 2017, 2018 and 2019. The experiment included three drip irrigation treatments under film mulching conditions, i.e., WF (full irrigation), WM (medium irrigation, 70%WF), WL (low irrigation, 40%WF). Results showed the normalized root mean square errors (NRMSEs) for soil water storage (SWS), soil temperature at 0, 5, 10, 20 cm soil depths, leaf area index (LAI), aboveground dry biomass (ADB) and yield under different irrigation treatments for the three seasons by the modified model were 14.8%, 43.5% (an averaged value for the 4 soil depths), 70.5%, 56.4% and 82.1% lower than those of the original model, respectively, which demonstrated higher simulation accuracy of the modified model for mulched field. The modified model could more accurately depict the changes of the SWS and LAI caused by the film mulching at various growth stages. It could also reveal the enhanced soil temperature by film mulching especially at the early stage (0–60 day after sowing (DAS)). We analyzed the film mulching effects by comparing the simulation results of the modified model and the original model which could represent the difference between film mulching and no mulching. Results showed that soil evaporation and evapotranspiration under film mulching conditions were 60.7% and 10.1% lower while crop transpiration was 20.2% higher compared with no mulching. The yield and water use efficiency (WUE) under film mulching conditions improved by 38.9% and 54.3% compared with no mulching. Film mulching had more significant influence on the SWS, LAI, ADB, yield, crop transpiration and WUE under WL treatment than under WF and WM treatments.

1. Introduction

Agriculture in arid region is greatly restricted by the shortage of water resources, where efficient use of irrigation water is crucial for the sustainable development of agriculture and economy (Karthe et al., 2014; Yang et al., 2018). Plastic film mulching is a technology of saving water, regulating soil temperature and increasing production that has been widely employed in the arid and semi–arid areas of the world (Maurya and Lal, 1981; Anikwe et al., 2007; Bonachela et al., 2012; Dong et al., 2014; Fan et al., 2019). In China, plastic film mulching with drip irrigation has been employed over 4.7 million hm^2 and applied in the cultivation of more than 40 crop types, including major field crops such as wheat, maize and cotton (He et al., 2018).

In the cultivation and production of field crops, soil moisture and soil temperature are key factors due to their direct impacts on crop growth and yield (Ramakrishna et al., 2006; Balashov et al., 2014). Soil water is mainly affected by precipitation, irrigation schedule, soil evaporation and root water uptake (Zhao et al., 2018; Li et al., 2020). Water stress in root zone limits crop transpiration, and affects the accumulation and distribution of dry matter and the crop yield (Du et al.,

* Corresponding author at: Center for Agricultural Water Research in China, China Agricultural University, No 17 Qinghua East Road, Haidian District, Beijing 100083, China.
E-mail addresses: maoxiaomin@cau.edu.cn, maoxiaomin@tsinghua.org.cn (X. Mao).

https://doi.org/10.1016/j.agrformet.2020.108127
Received 31 December 2019; Received in revised form 26 July 2020; Accepted 3 August 2020
Available online 18 August 2020
0168-1923/

2005). Soil temperature is a comprehensive indicator of soil thermal status, which influences crop phenology and canopy development, dry matter accumulation and yield formation (Stone et al., 1999).

Many field experiments were conducted to quantity the influence of film mulching on soil moisture and temperature status and crop growth (Alliaume et al., 2016; Fan et al., 2016; Yang et al., 2018). Plastic film mulching could reduce soil evaporation and increase rainwater detention, thus increase soil water storage (Chakraborty et al., 2010; Li et al., 2013). Plastic film mulching could also reduce soil water storage because the vigorous crop growth under film mulching consumed more water during the crop–growing seasons (Zhang et al., 2017c; Yang et al., 2018). Soil temperature was influenced by film mulching because of the change in albedo, the heat conduction on soil surface and the latent heat consumption (Liakatas et al., 1986). The transparent film mulching increased soil temperature at 0–10 cm and 10–20 cm depths by 2 °C and 3 °C, respectively (Fan et al., 2016). Film mulching provided favorable soil water and heat conditions for crop growth (Ren et al., 2008; Chen et al., 2015) and it could improve dry biomass and yield of maize by 21.0%–40.6% and 28.3%–87.5%, respectively (Bu et al., 2013). Therefore it is necessary to involve and accurately evaluate film mulching impacts in quantification of soil water and heat dynamics as well as their interactions with crop growth and yield.

Crop models are powerful tools to predict crop growth and yield under various agricultural management measures. Soil–Water–Atmosphere–Plant (SWAP) model, an agro–hydrological model, could simulate crop growth, vertical transport of water, solute and heat in both unsaturated and variably saturated soils (Kores et al., 2000). SWAP model reveals the close interactions between soil water/salt transport and crop growth (Van Dam et al., 2008). It has been proved that it could well simulate the transport of soil water and salt dynamics, crop growth and water consumption under various saline water irrigation scenarios at field scale (Jiang et al., 2011; Kumar et al., 2015; Kamyab–Talesh et al., 2017; Yuan et al., 2019). Good performance in predicting soil temperature was recorded for SWAP model in Balashov et al. (2014). SWAP model was also applied at regional scale, e.g. by assimilating leaf area index (LAI) and evapotranspiration/satellite–based surface incoming solar radiation into SWAP for crop yield estimation (Huang et al., 2015; Mokhtari et al., 2018), or by integrating SWAP and MODFLOW–2000 for simulation of regional groundwater dynamics (Xu et al., 2011b). In addition, SWAP model was used for predicting the impact of climate change on crop production and water productivity (Crescimanno et al., 2012; Martínez-Ferri et al., 2013; Liu et al., 2019).

Despite the large contributions SWAP had made on simulations under various agricultural managements and environmental scenarios, it was not particularly designed to deal with the impact of film mulching on crop growth. In general, impact of plastic film mulching was mostly considered by adjusting the input parameters or by modifying the crop model code. For example, in view of the warming and interception effect of plastic film, Kim et al. (2014) adjusted meteorological input data of precipitation and air temperature to consider the effects of plastic mulch on soil moisture and temperature dynamics based on LandscapeDNDC model. Yang et al. (2015) adjusted artificially the air temperature by considering the compensation effect of soil temperature on air temperature under film mulching to simulate the growth of mulched maize based on Aquacrop model. Han et al. (2014) and Liang et al. (2017), in Denitrification–Decomposition model (DNDC) and soil Water Heat Carbon Nitrogen Simulator model (WHCNS) respectively, considered the reduction of soil evaporation by the linear influence of the ratio of the ground covering film on the potential evaporation, and the increase of soil temperature considering the thickness and heat conductivity of the film. Hou et al. (2014) modified the Hybrid–Maize model by deducting soil evaporation linearly and using measured temperature beneath plastic film at 5 cm depth for simulating crop development and growth before the 6–leaf stage (V6). However, these studies did not comprehensively consider the effects of film mulching on soil water and heat status and their impact on crop growth, as well as not validating the performance of their models under various irrigation levels. Therefore, further work is required regarding the response of soil water and heat under film mulching and their comprehensive impacts on crop development under various irrigation levels.

In this study, SWAP model was adopted as the target model for modification, to accommodate the impact of film mulching on soil water and heat dynamics as well as crop growth and yield. Then, the performance of modified SWAP model was evaluated on the soil water storage (SWS), soil temperature, LAI, aboveground dry biomass (ADB), yield, water balance components and water use efficiency (WUE) under various irrigation levels based on our experimental data at seed–maize fields.

2. Field experiments

2.1. Experimental site description

The field experiments were conducted at Shiyang Experimental Station for Water–saving in Agriculture and Ecology of China Agricultural University, Wuwei City, Gansu Province of China (37°52′N, 102°52′E, elevation above mean sea level 1581 m). The mean annual precipitation is 164 mm and the mean annual pan evaporation is 2000 mm. Moreover, the average annual duration of sunshine is 3000 h, the mean annual air temperature is 8 °C and the mean annual air cumulative temperature (> 0 °C) is 3550 °C (He et al., 2018; Qin et al., 2018). The groundwater table is 40–50 m below the ground surface.

2.2. Experimental design

Seed–maize was planted in 137.2 m^2 plots (24.5 m in length and 5.6 m in width) with a row spacing of 40 cm and plant spacing of 25 cm. The planting date was April 24, April 20, April 18 in 2017, 2018, 2019, respectively. For convenience, in this study we divided the whole growing period of seed–maize into three stages, i.e., early stage (0–60 day after sowing (DAS)), middle stage (61–106 DAS) and late stage (after 107 DAS). The soil type in the field is silt loam and the measured soil physical properties along the soil profile are shown in Table 1. The farmland was covered by transparent plastic film of 85 cm wide and 0.004 cm thick, with 5 cm overlap in the adjacent films. The study

Table 1
Measured soil physical properties along the soil profile in the experiment site.

Soil layers (cm)	Particle fraction (%)			Bulk density (g cm^{-3})	Soil texture (USDA)
	Sand (2–0.05 mm)	Silt (0.05–0.002 mm)	Clay (<0.002 mm)		
0–20	27.1	63.6	9.3	1.53	Silt loam
20–40	30.2	60.4	9.4	1.48	Silt loam
40–60	17.9	71.1	11.0	1.46	Silt loam
60–80	17.0	73.0	10.0	1.58	Silt loam
80–100	35.2	57.1	7.7	1.50	Silt loam

Table 2
Irrigation schedule under different treatments in 2017, 2018 and 2019.

Treatments	2017				2018				2019			
	DAS (d)	Depth (mm)			DAS (d)	Depth (mm)			DAS (d)	Depth (mm)		
		WF	WM	WL		WF	WM	WL		WF	WM	WL
Irrigation schedule	37	15.0	10.5	6.0	43	14.5	10.2	5.8	45	14.8	10.4	5.9
	49	7.6	5.3	3.1	53	22.2	15.6	8.9	55	31.4	22.0	12.6
	57	39.7	27.8	15.9	62	40.2	28.2	16.1	65	35.0	24.5	14.0
	67	42.7	29.9	17.1	74	40.5	28.4	16.2	75	25.0	17.5	10.0
	77	42.1	29.4	16.8	84	37.9	26.5	15.1	85	24.0	16.8	9.6
	83	25.6	17.9	10.3	94	40.6	28.4	16.2	94	40.5	28.4	16.2
	87	30.3	21.2	12.1	104	50.2	35.2	20.1	105	43.1	30.2	17.2
	107	42.0	29.4	16.8	123	32.8	23.0	13.1	115	33.7	23.6	13.5
	127	61.3	42.9	24.5					125	41.3	28.9	16.5
Total depth (mm)		306.4	214.5	122.6		279.0	195.3	111.6		288.8	202.2	115.5

Note: DAS, day after sowing; WF, full irrigation; WM, medium irrigation, 70%WF; WL, low irrigation, 40%WF.

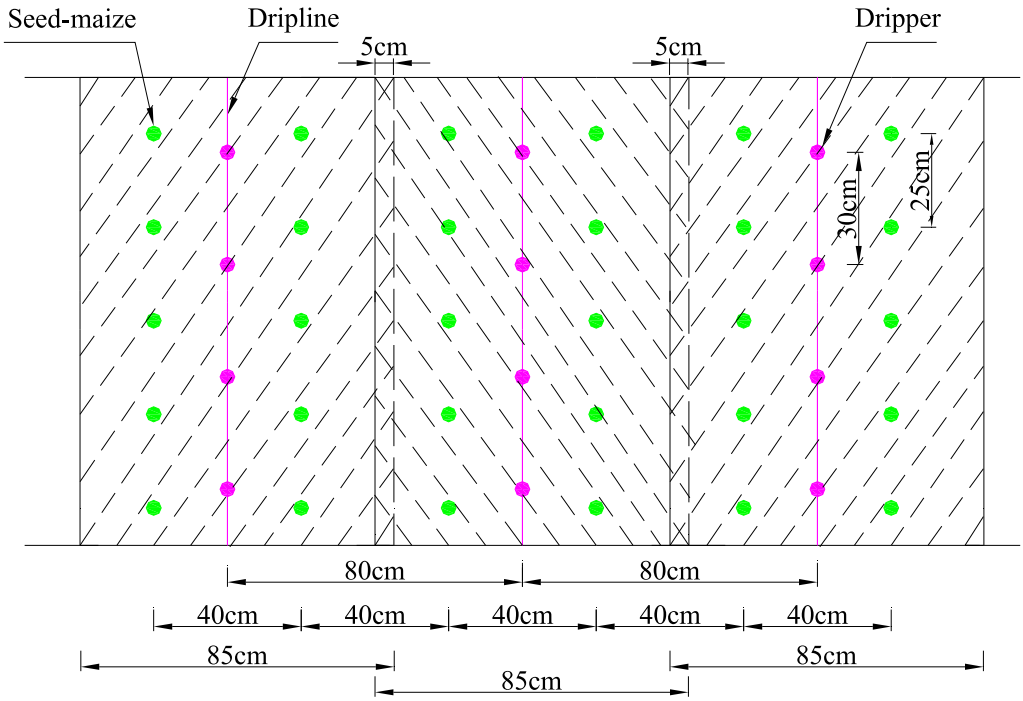

Fig. 1. Layout of the plastic film mulching, drip irrigation system and seed–maize.
Note: Three pieces of plastic film were shown in the figure in dashed lines, each with the width of 85 cm and 5 cm overlap between two adjacent films.

included three drip irrigation treatments, i.e., WF (full irrigation), WM (medium irrigation, 70%WF), WL (low irrigation, 40%WF) and the irrigation schedule is given in Table 2. The drip line was placed between two rows of seed–maize with a spacing of 80 cm. Drippers were located every 30 cm along the drip line and the discharge rate was 2.5 L h^{-1}. The layout of the film mulch, drip irrigation system and seed–maize are shown in Fig. 1.

2.3. Field data collection

The volumetric water content of the soil was measured every 3–7 d at 20 cm intervals from the surface to the depth of 100 cm using Time–Domain–Reflectometry (TRIME–PICO/PICO–BT, Imko GmbH, Ettlingen, Germany). The soil temperature at the depths of 0, 5, 10, 20 cm was monitored every 30 min (except the soil temperature at 5 cm depth in 2017) by the temperature sensors connected with soil temperature recorders (HZ–TJ1, both sensors and recorders came from Hezhong Bopu Technology Development Co., Ltd., Beijing, China). A ruler was used to measure the length and maximum width of fully unfolded leaves every 7–10 d to get LAI. The ADB was measured by drying the whole plant sampled randomly from the plot every 15–20 d. At maturity, the 10 consecutive seed–maize ears were hand–harvested from the center of each plot to measure the seed–maize yield, which was expressed at a water content of 12% (Li et al., 2013; Ren et al., 2017). Although no replicate treatment was considered due to the limitations of the field experimental plot, soil water content, LAI, ADB and yield were measured at three locations in each plot.

3. SWAP model and modifications

3.1. Introduction of SWAP model

SWAP, coded in FORTRAN, was developed by the Water Resources Group of Wageningen University and is an physically based and detailed agro–hydrological model Kroes et al., 2000). SWAP provides two or more options in some modules, such as for the soil hydraulic characteristics, water stress function, soil heat flow and crop growth process, etc. In this study, soil water flow in saturated and unsaturated zone was described by Richards equation (Richards, 1931), with van Genuchten–Mualem (VGM) model (van Genuchten, 1980) to show the soil hydraulic property (i.e., the relationship between soil matric potential, water content and the unsaturated hydraulic conductivity), and

Feddes model (Feddes et al., 1978) to show root water extraction. The VGM model can be expressed by Eqs. (1)–((3) (van Genuchten, 1980). Soil heat flow was described by heat conduction equation. Crop growth was predicted by a detailed crop model (WOFOST) (Boogaard et al., 1998), taking into account growth reductions due to water and oxygen stresses. More detailed descriptions of the model could be found in the user manual of SWAP version 4.0 (Kroes et al., 2017).

$$\theta(h) = \begin{cases} \theta_r + \dfrac{\theta_s - \theta_r}{(1 + |\alpha h|^n)^m} & (h < 0) \\ \theta_s & (h \geq 0) \end{cases} \quad (1)$$

$$K(h) = K_s S_e^{\lambda}[1 - (1 - S_e^{1/m})^m]^2 \quad (2)$$

$$S_e = \frac{\theta - \theta_r}{\theta_s - \theta_r} \quad (3)$$

where θ is volumetric water content (cm^3cm^{-3}), h is soil water pressure head (cm), θ_s is saturated water content (cm^3cm^{-3}), θ_r is residual water content (cm^3cm^{-3}), α is an empirical parameter (cm^{-1}), n, m and λ are empirical shape factors, and $m = 1/(1 - n)$, K is unsaturated hydraulic conductivity (cm d^{-1}), K_s is saturated hydraulic conductivity (cm d^{-1}), S_e is effective saturation.

3.2. Modifications of SWAP model

3.2.1. Basis for model modifications

Our previous work on comparison of experimental results of farmland with and without film mulching (Zhao et al., 2018) demonstrated that transparent plastic film mulching could block rainfall infiltration, reduce soil evaporation, regulate soil temperature and accelerate crop growth and development. This provided fundamental support for the model modifications in this work. We also referred to previous studies (Dong et al., 2014; Fan et al., 2016; Yang et al., 2018) for the reliability of our model modifications. Based on the above analysis, the soil moisture module, soil temperature module and crop growth module in SWAP were modified respectively in this study.

3.2.2. Modification of soil temperature module

In the original SWAP model, the upper boundary condition of soil heat flow was Dirichlet boundary by specifying the upper boundary temperature. The bottom boundary condition could be Dirichlet boundary by specifying the bottom boundary temperature or Neumann boundary by specifying zero heat flux. With no direct measurements of soil surface temperature, normally users could only use air temperature as the upper boundary condition. With film mulching, it can significantly modify the relationship between the soil surface temperature and air temperature.

To make SWAP model more applicable under film mulching conditions when without monitored soil temperature, we firstly calculated the soil surface temperature under non–mulched soil. Zheng et al. (1993) demonstrated that there was difference in the estimation of soil surface temperature under non–mulched soil between crop cover and no crop cover. In this study, when the LAI was less than 1 cm^2cm^{-2} (LAI < 1), the soil surface temperature under non–mulched soil was obtained by establishing a regression equation (Eq. (4)) for the measured soil surface temperature without mulching on the current day (T_{top}, °C) and previous day (T_{top}', °C), as well as the air temperature on the current day (T_{air}, °C) and previous day (T_{air}', °C), with a high correlation coefficient of 0.865.

$$T_{top} = 1.048T_{air} - 0.311T_{air}' + 0.313T_{top}' + 0.413 \quad (4)$$

When the LAI was not less than 1 cm^2cm^{-2} (LAI ≥ 1), the soil surface temperature under non–mulched soil was obtained based on T_{top}', T_{air} and LAI (Eq. (5)) (Zheng et al., 1993).

$$T_{top} = \begin{cases} T_{top}' + 0.25(T_{air} - T_{top}')\exp(-k_e LAI) & (T_{air} \geq T_{top}') \\ T_{top}' + 0.25(T_{air} - T_{top}') & (T_{air} < T_{top}') \end{cases} \quad (5)$$

where k_e is the light extinction coefficient and is the product of extinction coefficient for diffuse visible light (K_{dif}) and the extinction coefficient for direct visible light (K_{dir}). K_{dif} and K_{dir} need to be specified by the user.

And then the soil surface temperature under film mulching conditions (T_{ftop}, °C) was determined by the T_{air}, daily maximum air temperature (T_{max}, °C) and T_{top}, as well as by the film thickness (D_{film}, cm) and the thermal conductivity (TC_{film}, J cm^{-1} °$C^{-1}d^{-1}$) Ma et al., 2015) as shown in Eqs. (6) and ((7). Liang et al. (2017) showed that the effect of film mulching on soil temperature was mainly at the stage of LAI < 1, while little effect at the stage of LAI ≥ 1. Therefore, the Eqs. (6) and (7) was solely applied at the stage of LAI < 1, while T_{ftop} was set equal to T_{top} at the stage of LAI ≥ 1.

$$dH = \left(\frac{T_{air} + T_{max}}{2} - T_{top}\right) \cdot D_{film} \cdot TC_{film} \cdot dt \quad (6)$$

$$T_{ftop} = T_{top} + \frac{dH}{C_{soil}\, dV} \quad (7)$$

where dH is heat flux from the film surface to the soil surface (J), C_{soil} is the soil specific heat capacity (J cm^{-3} °C^{-1}), t is the unit of time (d), dV is set to 1 cm^3.

For the bottom boundary condition, with no direct measurements of the bottom soil temperature, normally the users could only take zero heat flux as the bottom boundary condition. Because the bottom depth in our study was 100 cm, zero heat flux assumption was unsuitable. In order to specify a more appropriate bottom boundary condition under no direct measurement, we used a common approach Eqs. (8) and ((9)) for estimating the bottom soil temperature (Zhang et al., 2002).

$$T_{bot} = T_{mean} + T_{ampl} \exp\left(\frac{Z}{d_{demp}}\right) \cos\left(\frac{2\pi}{365}(JD - JD_0) + \frac{Z}{d_{demp}}\right) \quad (8)$$

$$d_{demp} = \sqrt{\frac{2\lambda_a / C_a}{2\pi / 365}} \quad (9)$$

where T_{bot} is the soil temperature (°C) at the depth of Z (100 cm), T_{mean} is the mean annual air temperature (°C), T_{ampl} is the amplitude of air temperature (°C), d_{demp} is the damping depth (cm), JD is the day of the year (DoY), JD_0 is the DoY when the air temperature reaches its maximum, λ_a is the average thermal conductivity of the soil profile (J cm^{-1} °$C^{-1}d^{-1}$), C_a the average heat capacity of the soil profile (J cm^{-3} °C^{-1}).

3.2.3. Modification of soil water module

In SWAP, the bottom boundary condition of the soil water movement was specified as free drainage. The upper boundary condition was Neumann boundary determined by irrigation, precipitation and evaporation. When drip irrigation was applied, the soil surface was assumed to be completely wet so that it could be simplified as 1–D vertical soil water movement. For precipitation, the canopy interception (ΔP_c, mm d^{-1}) was described by Hoyningen–Braden method (Hornung and Messing, 1983; Braden, 1985),

$$\Delta P_c = a \cdot LAI \left[1 - \frac{1}{1 + (b \cdot P)/(a \cdot LAI)}\right] \quad (10)$$

$$b = 1 - \exp(-k_e LAI) \quad (11)$$

where a is an empirical coefficient (mm d^{-1}) and should be specified by the users, b is the soil cover fraction, P is the total precipitation (mm d^{-1}).

Under plastic film mulching conditions, in addition to canopy interception, the film interception on precipitation should also be considered. Haraguchi et al. (2003) concluded about 80% of the

precipitation infiltrated into the soil through transplanting holes under full film mulching and infiltration into holes might occur because the water could flow in all directions due to the flat surface. Therefore, film interception was considered to be 20% in our study and the precipitation interception (ΔP, mm d^{-1}) including canopy and film interception was calculated by Eq. (12),

$$\Delta P = \Delta P_c + (P - \Delta P_c)\cdot 20\% \tag{12}$$

In this study, the potential evaporation (E_p, mm d^{-1}) and transpiration (T_p, mm d^{-1}) was calculated by direct application of Penman–Monteith (Kores et al., 2017),

$$T_p = \frac{(1 - W_{frac})\left[b\frac{\Delta_v}{\lambda_w}(R_n - G) + \frac{p_1\rho_{air}C_{air}}{\lambda_w}\left(\frac{e_{sat} - e_a}{r_{air,can}}\right)\right]}{\Delta_v + \gamma_{air}\left[1 + \frac{r_{s,min}}{r_{air,can}LAI_{eff}}\right]} \tag{13}$$

$$E_p = \frac{(1 - b)\frac{\Delta_v}{\lambda_w}(R_n - G) + \frac{p_1\rho_{air}C_{air}}{\lambda_w}\left[\frac{e_{sat} - e_a}{r_{air,soil}}\right]}{\Delta_v + \gamma_{air}\left[1 + \frac{r_{soil}}{r_{air,soil}}\right]} \tag{14}$$

$$LAI_{eff} = \frac{LAI}{0.3LAI + 1.2} \tag{15}$$

where W_{frac} is the fraction of the day in which the canopy is wet, Δ_v is the slope of the vapor pressure curve (kPa °C^{-1}), λ_w is the latent heat of vaporization (J kg^{-1}), R_n is the net radiation flux at the canopy surface (J m^{-2} d^{-1}), G is the soil heat flux (J m^{-2} d^{-1}), p_1 accounts for unit conversion (86,400 s d^{-1}) ρ_{air} is the air density (kg m^{-3}), C_{air} is the heat capacity of moist air (J kg^{-1} °C^{-1}), e_{sat} is the saturation vapor pressure (kPa), e_a is the actual vapor pressure (kPa), $r_{air,can}$ is the aerodynamic resistance of uniform crop (s m^{-1}), γ_{air} is the psychrometric constant (kPa °C^{-1}), $r_{s,\ min}$ is the minimal stomatal resistance (s m^{-1}), LAI_{eff} is the effective leaf area index, $r_{air,soil}$ is the aerodynamic resistance of soil surfaces, r_{soil} is the soil resistance of a wet soil (s m^{-1}). Note that on a daily base, G is assumed to be negligible in SWAP. The calculation method of each parameter in this equation was introduced in detail in Kroes et al. (2017), not described here. For the users, main parameters need to be given include crop height (*CH*), crop reflection coefficient (albedo) and minimum canopy resistance (*MCR*). The measured *CH* was given, and the albedo and *MCR* took the model default as the original value.

In SWAP, soil evaporation was also calculated according to Darcy's law (Eq. (16)) and the empirical function (Eq. (17)).

$$E_{max} = k_{1/2}\left(\frac{h_{atm} - h_1 - Z_1}{Z_1}\right) \tag{16}$$

where E_{max} is the maximum evaporation rate (mm d^{-1}), $k_{1/2}$ is the average hydraulic conductivity between the soil surface and the adjacent discretization node (node 1) in soil (mm d^{-1}), h_{atm} is the soil water pressure head in equilibrium with the air relative humidity (cm), h_1 is the soil water pressure head of the first node (cm), Z_1 is the soil depth at node 1 (cm).

$$\sum E_a = \beta t_{dry}^{1/2} \tag{17}$$

where ΣE_a is the cumulative actual evaporation (mm), β is a soil–specific parameter (mm $d^{-1/2}$) characterizing the evaporation process, t_{dry} is the time after a significant amount of rainfall (d).

In original SWAP, soil evaporation (E, mm d^{-1}) was determined by taking the minimum value of E_p, E_{max}, and ΣE_a,

$$E = \min(E_p, E_{max}, E_a) \tag{18}$$

In this study, planting holes existed despite the application of full film mulching. Qin et al. (2018) concluded the proportion of planting holes was 2.13% which applied the same cultivation technology as ours. Wu et al. (2017) showed that the soil evaporation from planting holes could not be ignored under film mulching conditions. Li (2002), based on the same soil type and irrigation method (drip irrigation) as ours, indicated that the relationship between the reduction rate of soil evaporation under film mulching conditions (C_{film}) and the opening holes ratio (δ) could be expressed by Eq. (19),

$$C_{film} = 1 - \delta^{0.2047} \tag{19}$$

When δ is 2.13%, C_{film} is 55%. Therefore, in our study, the coefficient C_{film} with original (i.e., before calibration) value of 55% was introduced, which showed the reduction rate of soil evaporation under film mulching to that of non–mulched soil. In the modified SWAP, soil evaporation (E_{pfilm}, $E_{maxfilm}$, E_{afilm}, E_{film}) under film mulching was calculated by Eqs. (20)–(23),

$$E_{pfilm} = (1 - C_{film})\cdot E_p \tag{20}$$

$$E_{maxfilm} = (1 - C_{film})\cdot E_{max} \tag{21}$$

$$E_{afilm} = (1 - C_{film})\cdot E_a \tag{22}$$

$$E_{film} = \min(E_{pfilm}, E_{maxfilm}, E_{afilm}) \tag{23}$$

3.2.4. Modification of crop growth module

In the original SWAP model, all crop physiological processes were simulated based on air temperature, including phenological development stages and photosynthesis and respiration. The crop development stage D_s was obtained by Eqs. (24) and (25),

$$D_s(JD + 1) = D_s(JD) + \frac{T_{eff}}{T_{sum,i}} \tag{24}$$

$$T_{eff} = \begin{cases} 0 & (T_{air} < T_b) \\ T_{air} - T_b & (T_b \le T_{air} \le T_0) \\ T_0 - T_b & (T_{air} > T_0) \end{cases} \tag{25}$$

where $D_s(JD+1)$ and $D_s(JD)$ are the crop development stage when DoY is $JD+1$ and JD respectively, T_{eff} is the effective temperature (°C), $T_{sum,i}$ is the temperature sum (°C) required to complete either the vegetative or the reproductive stage and given by the user, T_b is base point temperature (°C), T_0 is optimum temperature (°C). T_b and T_0 are 8 °C and 34 °C for maize, respectively (Jones and Kiniry, 1986).

The crop development rate was not always dependent on the air accumulated temperature, but was controlled by the temperature of the meristem Ma et al., 2017). Stone et al. (1999) concluded maize meristem was underground before V6 (6–leaf stage) and the crop development rate was affected by the soil temperature. Under the conditions of plastic film mulching, the soil temperature increased significantly at the early stage of crop growth, and large error in crop growth simulation would occur if the prediction was based on air accumulated temperature (Hou et al., 2014; Ma et al., 2017). Therefore, SWAP model was modified to employ soil temperature at a depth of 5 cm below the plastic film for simulation of crop development stage ($D_{s–film}$) before V6 by Eqs. (26) and ((27), while air temperature was still used for physiological processes including photosynthesis and respiration.

$$D_{s-film}(JD + 1) = D_{s-film}(JD) + \frac{T_{eff-film}}{T_{sum,i}} \tag{26}$$

$$T_{eff-film} = \begin{cases} 0 & (T_{soil5} < T_b) \\ T_{soil5} - T_b & (T_b \le T_{soil5} \le T_0) \\ T_0 - T_b & (T_{soil5} > T_0) \end{cases} \tag{27}$$

where $D_{s–film}(JD+1)$ and $D_{s–film}(JD)$ are the crop development stage under film mulching conditions when DoY is $JD+1$ and JD respectively, $T_{eff–film}$ is the effective temperature before V6 under film mulching (°C), T_{soil5} is the soil temperature at 5 cm depth (°C).

3.3. Model input parameters

3.3.1. Meteorological and irrigation data

The meteorological data required by the SWAP model mainly included daily solar radiation, maximum temperature, minimum temperature, precipitation, humidity and wind speed, which were measured using a standard automatic weather station (Hobo, Onset Computer Corp, USA) at a height of 2.0 m above the ground from 2017 to 2019. The irrigation data was specified based on the actual irrigation schedule as Table 2.

3.3.2. Soil parameters

Soil parameters mainly included soil hydraulic parameters, soil evaporation parameters and soil heat transfer parameters. The original soil hydraulic parameters, as those parameters in VGM model, were obtained by available soil textural information (i.e., the measured soil particle composition and dry bulk density in Table 1) through the neural–network–based pedotransfer function approach (Šimůnek et al., 1999). The original soil evaporation parameters were specified as the model default value (β) or based on the previous study (C_{film}). Soil heat transfer parameters required from the user mainly included soil texture information for the heat conduction equation and the parameters (D_{film}, TC_{film}, T_{mean}, T_{ampl}) for the estimation of upper and bottom soil temperature in the modified model. The original soil texture, D_{film}, T_{mean}, T_{ampl} were given from the measured value and the original TC_{film} were selected from Kroes et al. (2017). The above parameters were then calibrated in modified SWAP based on the experimental data.

3.3.3. Crop parameters

The crop module in SWAP, i.e., WOFOST, contained many crop parameters such as crop development, initial leaf area index and total dry weight, green surface area, assimilation, conversion of assimilation into biomass, maintenance respiration, partitioning, death rates, root growth, etc. The original values of these parameters were given from the measured values or model default values.

3.4. Parameter sensitivity analysis and model calibration

SWAP model was calibrated using monitored data in the experiment of 2017 and validated by that of 2018 and 2019, respectively. SWAP involved so many parameters that increased the difficulty of calibration and possibly resulted in overfitting. Therefore, only the high sensitivity parameters were calibrated to achieve the highest efficiency of the SWAP model in predicting SWS, soil temperature, LAI, ADB and yield.

In this study, the sensitivity of model parameters was investigated by one–at–a–time (OAT) method (Ma et al., 2013). The model was run with change in the value of one input parameter at a time by 10% increase and then by 10% decrease of its original value. Only one parameter of the model was changed and the others were fixed at every model run, and all parameters repeated the same process to investigate the impact of the change on the simulation results of SWS, LAI, ADB, yield and soil temperature. The relative sensitivity (*RS*) (Wilkerson et al., 1983) was used to express the sensitivity as follows,

$$RS = \left| \frac{(y(x + \Delta x) - y(x))/y(x)}{\Delta x/x} \right| \quad (28)$$

where x is a parameter value in the model parameter, Δx is the change of the parameter, $y(x)$ and $y(x + \Delta x)$ respectively represent the output value before and after the parameter change, including SWS, LAI, ADB, yield and soil temperature. The higher *RS* value is, the more sensitive the parameter is, and vice versa.

3.5. Model evaluation statistics

Three statistical indices were used to evaluate model performance, i.e., root mean square error (RMSE), normalized root mean square error (NRMSE) and coefficient of determination (R^2).

$$RMSE = \sqrt{\frac{\sum_{i=1}^{i=N} (M_i - S_i)^2}{N}} \quad (29)$$

$$NRMSE = \frac{\sqrt{\frac{\sum_{i=1}^{i=N} (M_i - S_i)^2}{N}}}{\bar{M}} \quad (30)$$

$$R^2 = \frac{\left[\sum_{i=1}^{i=N} (M_i - \bar{M})(S_i - \bar{S})\right]^2}{\sum_{i=1}^{i=N} (M_i - \bar{M})^2 \sum_{i=1}^{i=N} (S_i - \bar{S})^2} \quad (31)$$

where *M, S*, $\bar{M}$, $\bar{S}$, and *N* are the measured values, the simulated values, the mean of measured values, the mean of simulated values, and the number of measured values, respectively. Note that the lower the RMSE and NRMSE values and the higher R^2, the better the simulation effect (Jamieson et al., 1991).

4. Results

4.1. The results of sensitivity analysis and model calibration

Parameters with *RS* greater than 0.1 are listed and arranged in the order of *RS* reduction in Table 3. Crop parameters had a higher sensitivity than soil hydraulic parameters, and *RS* for soil temperature parameters was the lowest. In addition, the sensitivity of soil temperature parameters (D_{film}, TC_{film}) to crop growth (LAI, ADB, yield) was greater than 0.1, demonstrating soil temperature parameters should be calibrated before crop parameters. Therefore, the order of the parameter calibration was set up as soil temperature parameters, followed by crop parameters and soil hydraulic parameters. The results of parameter calibration are given in Tables 4–6.

4.2. Model performance

4.2.1. Soil water storage (SWS)

The measured and simulated SWS by the original and modified models are shown in Fig. 2. The SWS by the modified model was more consistent with the measured SWS than that of the original model. Table 7 showed that the simulation accuracy of SWS was better by the modified model. Compared with the original model, RMSEs (or NRMSEs) of SWS under different irrigation treatments for the three seasons by the modified model decreased by 5.1%–26.4% (i.e., the range of all values under the different irrigation treatments for the three seasons) except for WL treatment in 2017 and WM treatment in 2018. The average R^2 was 0.81 and 0.70 by the modified and original models, respectively. The modified model performed better for the SWS during the various growing stages than the original model, except for the middle stage under WL treatment in 2017, 2018, 2019 and the late stage under WM treatment in 2018. The RMSE by the modified model was averagely 26.1%, 20.3%, 21.6% lower at the early, middle, late stages than that of the original model, respectively. In this study, film mulching effect was included in the modified model, while the original model demonstrated the case where there was no film mulching effect under the same input conditions as the modified model. Therefore, we could assume that the comparison between modified and original models represented the difference between the film mulching and no mulching. Comparing the SWS of the modified model with that of the original model, we could see the average SWS at the early stage for the three seasons by the modified model was 4.8% (i.e., the averaged value of the three seasons), 5.6%, 7.6% higher under WF, WM, WL treatments than that of the original model (Fig. 2). The average SWS at the middle stage for the three years by the modified model was 3.9%, 4.6%, 6.8% lower under WF, WM, WL treatments than that of the original model. It indicated that film mulching (as represented by the simulation results

Table 3
The relative sensitivity (*RS*) of model parameters for SWS, LAI, ADB, yield and soil temperature.

Output	SWS	LAI	ADM	Yield	Soil temperature
Parameters	n (0.340)	T_{sum1} (1.427)	*LUE* (0.952)	T_{sum2} (1.457)	D_{film} (0.102)
	ρ (0.332)	*LUE* (0.892)	*EC–R* (0.665)	*LUE* (0.989)	TC_{film} (0.102)
	θ_s (0.295)	*SPAN* (0.816)	*EC–L* (0.632)	*SPAN* (0.962)	Soil texture (0.101)
	C_{film} (0.243)	*MRILAI* (0.766)	*MRILAI* (0.575)	T_{sum1} (0.931)	
	β (0.204)	*EC–L* (0.709)	A_{max} (0.565)	*EC–SO* (0.695)	
	α (0.104)	*FTADM–R* (0.589)	*FTDM–R* (0.557)	*EC–S* (0.317)	
		SLA (0.588)	*EC–S* (0.502)	*SLA* (0.302)	
		EC–R (0.581)	*ITCDW* (0.475)	*FTDM–S* (0.292)	
		ITCDW (0.548)	*SLA* (0.416)	K_{dif} (0.232)	
		EC–S (0.499)	*FTDM–L* (0.309)	*MRR–L* (0.201)	
		FTDM–L (0.426)	D_{film} (0.302)	*MRILAI* (0.172)	
		D_{film} (0.349)	TC_{film} (0.302)	A_{max} (0.156)	
		TC_{film} (0.349)	K_{dif} (0.252)	*EC–L* (0.154)	
		A_{max} (0.269)	T_{sum1} (0.157)	D_{film} (0.128)	
		K_{dif} (0.264)	*MRR–L* (0.120)	TC_{film} (0.128)	

Note: A_{max}, max CO_2 assimilation rate; C_{film}, reducing ratio of soil evaporation under film mulching; D_{film}, film thickness; *EC–L*, efficiency of conversion into leaves; *EC–R*, efficiency of conversion into roots; *EC–S*, efficiency of conversion into stems; *EC–SO*, efficiency of conversion into storage organs; *FTADM–L*, fraction of total aboveground dry biomass to the leaves; *FTADM–R*, fraction of total aboveground dry biomass to the roots; *FTADM–S*, fraction of total aboveground dry biomass to the stems; *ITCDW*, initial total crop dry weight; K_{dif}, extinction coefficient for diffuse visible light; *LUE*, light use efficiency; *MRILAI*, maximum relative increase in LAI; *MRR–L*, maintenance respiration rate of leaves; *SLA*, specific leaf area; *SPAN*, life span under leaves under optimum conditions; T_{sum1}, temperature sum from emergence to anthesis; $T_{sum\ 2}$, temperature sum from anthesis to maturity; TC_{film}, film thermal conductivity; n, shape factor for soil water retention curve; α, shape factor for soil water retention curve; ρ, dry soil bulk density; θ_s, saturated water content; β, soil–specific parameter; The values in parentheses after the parameters are their *RS*.

of the modified model) could enhance SWS at the early stage and decrease the SWS at the middle stage. Besides, with the decrease of irrigation amounts, both the enhancing effect and the decreasing effect were amplified.

4.2.2. Soil temperature

The measured and simulated soil temperature at the shallow soil layer (at 0, 5, 10, 20 cm soil depths) by the original and modified models are presented in Fig. 3. The variation trend of soil temperature by simulation and observation was similar. The measured soil temperature mostly fell on the curve of the modified model, especially at the early stage. Table 8 showed that the simulation accuracy of soil temperature by the modified model was improved, where the average RMSE, NRMSE, R^2 at different soil depths for the three seasons were 1.52 °C, 7.31%, 0.83 by the modified model and 2.59 °C, 12.49%, 0.68 by the original model. The simulation especially improved the accuracy at the early stage, where the average RMSE, NRMSE, R^2 at different soil depths for the three seasons were 1.74 °C, 8.51%, 0.89 by the modified model and 3.61 °C, 17.56%, 0.87 by the original model. While for the middle and late stages, the average RMSE, NRMSE, R^2 (1.28 °C, 6.07%, 0.83) of the modified model were close to that of the original model (1.48 °C, 7.09%, 0.82). Compared with the original model, the average RMSE (or NRMSE) of the soil temperature by the modified model decreased by 51.8% at the early stage, while at the middle and late stages decreased by 13.5%. In addition, for both the modified model and the original model, the soil temperatures at 20 cm depth had the smallest RMSE and NRMSE values except for the original model in 2019 and RMSE of the soil temperature at 20 cm depth was averagely 23.8%

Table 4
Main crop parameters used in SWAP.

Parameters	Descriptions	Initial values	Values	Source of initial values
T_{sum1}, °C·d	Temperature sum from emergence to anthesis	850	895	Measured
T_{sum2}, °C·d	Temperature sum from anthesis to maturity	800	780	Measured
ITCDW, kg ha^{-1}	Initial total crop dry weight	10	10	Measured
MRILAI, m^2 m^{-2} d^{-1}	Maximum relative increase in LAI	0.0294	0.02	Kores et al. (2017)
SLA, ha kg^{-1}	Specific leaf area (0–0.5–0.8–1–2)	0.0026–0.0017–0.0012–0.0012–0.0012	0.0035–0.0015–0.0007–0.0005–0.0005	Kores et al. (2017)
SPAN, d	Span	33	35	Kores et al. (2017)
K_{dif}, (–)	Extinction coefficient for diffuse visible light	0.60	0.60	Kores et al. (2017)
K_{dir}, (–)	Extinction coefficient for direct visible light	0.75	0.55	Kores et al. (2017)
A_{max}, kg ha^{-1} h^{-1}	Max CO_2 assimilation rate (0–1–1.5–2)	70–70–70–70	40–48–60–40	Kores et al. (2017)
EC–L, kg^{-1}	Efficiency of conversion into leaves	0.65	0.80	Cheng et al. (2016)
EC–SO, kg^{-1}	Efficiency of conversion into storage organs	0.82	0.60	Cheng et al. (2016)
EC–R, kg^{-1}	Efficiency of conversion into roots	0.72	0.70	Cheng et al. (2016)
EC–S, kg^{-1}	Efficiency of conversion into stems	0.69	0.80	Cheng et al. (2016)
MRR–L, kg CH_2O kg d^{-1}	Maintenance respiration rate of leaves	0.030	0.020	Kores et al. (2017)
FTADM–R, (–)	Fraction of total aboveground dry biomass to the roots (0–0.2–0.4–1–2)	0.40–0.34–0.27–0.00–0.00	0.55–0.44–0.33–0.00–0.00	Kores et al. (2017)
FTADM–L, (–)	Fraction of total aboveground dry biomass to the leaves (0–0.33–0.88–0.95–1.1–1.2–2)	0.62–0.62–0.15–0.15–0.40–0.00–0.00	0.60–0.60–0.60–0.60–0.00–0.00–0.00	Kores et al. (2017)
FTADM–S, (–)	Fraction of total aboveground dry biomass to the stems (0–0.33–0.88–0.95–1.1–1.2–2)	0.38–0.38–0.85–0.85–0.40–0.00–0.00	0.40–0.40–0.40–0.40–0.90–0.60–0.00	Kores et al. (2017)

Note: In the table, the values in parentheses of the second column refer to development stages where 0 is emergence, 1 is anthesis, 2 is maturity, and so on.

Table 5
Calibrated soil hydraulic parameters in van Genuchten–Mualem (VGM) model (van Genuchten, 1980).

Soil layers (cm)	Residual water content θ_r (cm^3cm^{-3})	Saturated water content θ_s (cm^3cm^{-3})	Saturated hydraulic conductivity K_s (cm d^{-1})	shape factor for soil water retention curve α (cm^{-1})	shape factor for soil water retention curve n (–)	Hydraulic conductivity shape factor λ (–)
0–20	0.04	0.41	20.84	0.0172	1.585	0.5
20–40	0.04	0.40	24.65	0.0169	1.597	0.5
40–60	0.08	0.43	25.77	0.0155	1.660	0.5
60–80	0.08	0.42	16.97	0.0169	1.594	0.5
80–100	0.03	0.42	25.41	0.0188	1.543	0.5

lower than that of the other soil depths (Table 8).

4.2.3. Leaf area index (LAI)

The measured and simulated LAI by the original and modified models are presented in Fig. 4. Generally, the simulation effect of the modified model on LAI was better than that of the original model under different irrigation treatments, especially in the rapid growth stage of seed–maize. During the whole growing period, RMSEs of LAI under different irrigation treatments for the three seasons by the modified model were 52.2%–83.9% lower than those of the original model (Table 9). R^2 were 0.91–0.99 and 0.79–0.98 by the modified and original models, respectively. At the early and middle stages, the RMSE of LAI under different irrigation treatments for the three seasons by the modified model reduced by 77.4% compared with the original model. The average R^2 were 0.99 and 0.90 by the modified and original models, respectively. While at the late stage, the RMSE of LAI under different irrigation treatments for the three years by the modified model for three years reduced by 25.9% compared with the original model, except for WF treatment in 2018 and 2019. The average R^2 were 0.98 and 0.94 by the modified and original models, respectively. Comparison between the modified and original models showed that the average LAI at the early and middle stages for the three years by the modified model was 12.7%, 27.5%, 47.9% higher under WF, WM, WL treatments than that of the original model (Fig. 4). It indicated that film mulching could increase LAI, and with the decrease of irrigation amount this effect was more prominent. It showed the beneficial effect of film mulching for maintaining LAI especially under deficit irrigation.

4.2.4. Aboveground dry biomass (ADB)

The simulated ADB by the modified model agreed better with the measured values than the original model (Fig. 5). RMSEs of ADB under different irrigation treatments for the three seasons by the modified model were 1.9%–72.5% lower than those of the original model except for WL treatment in 2017 (Table 10). Comparison between the modified and original models showed the average ADB during the entire growing period for the three seasons by the modified model was 17.5%, 24.1%, 33.3% higher under WF, WM, WL treatments than that of the original model (Fig. 5). It indicated film mulching could increase ADB and this effect was more prominent under deficit irrigation.

4.2.5. Water balance components, yield and water use efficiency (WUE)

Comparisons of the water balance components, yield and WUE of different treatments by the original and modified models are presented in Table 11. Precipitation and irrigation were the main water input and the irrigation amount of WF, WM, WL treatments accounted for 65.1%, 56.7%, 47.8% of the total water input, respectively. An average of 28.4% of precipitation was intercepted in the modified model, while only 9.1% in the original model. It was because plastic film interception was also considered in addition to canopy interception in the modified model. The average soil evaporation for the three seasons by the modified model was 56.0, 56.0, 58.2 mm under WF, WM, WL respectively, which was 61.1%, 61.2%, 59.8% less than that of the original model. The average crop transpiration for the three seasons by the modified model was 348.9, 309.1, 242.5 mm under WF, WM, WL respectively, which was 10.9%, 19.1%, 30.7% higher than that of the original model. The average evapotranspiration for the three seasons by the modified model was 11.7%, 9.7%, 8.9% lower under WF, WM, WL than that of the original model. A small amount of deep percolation occurred under WF treatment, while other treatments had no deep percolation.

The simulation performance of the seed–maize yield by the modified model was significantly improved compared with the result of the original model. NRMSEs of yield under different irrigation treatments for the three seasons were 0.88%–12.80% and 14.84%–46.71% by the modified and original models, respectively. NRMSEs of yield by the modified model averagely decreased by 82.1% compared with the original model.

Comparison of the results between the modified and original models showed that the yield for the three seasons by the modified model was 29.4%, 37.3%, 50.2% higher under WF, WM, WL treatments than that of the original model. The WUE for the three seasons by the modified model was 46.6%, 51.7%, 64.5% higher under WF, WM, WL treatments than that of the original model. It indicated that film mulching could improve the yield and WUE especially under deficit irrigations.

5. Discussion

5.1. Evaluation of modified model under film mulching conditions

5.1.1. Soil water module evaluation

In general, water consumption includes evapotranspiration, deep

Table 6
Other parameters used in SWAP.

Parameters	Descriptions	Initial values	Values	Source of initial values
C_{film}, (–)	Reduction rate of soil evaporation under film mulching	55%	60%	Li (2002)
β, mm $d^{-1/2}$	Soil–specific parameter for the evaporation process	3.5	5.0	Kores et al. (2017)
a, mm d^{-1}	Empirical coefficient for canopy interception	2.5	3.0	Kores et al. (2017)
D_{film}, cm	Film thickness	0.004	0.006	Measured
TC_{film}, J cm^{-1} $^{\circ}C^{-1}d^{-1}$	Film thermal conductivity	216	216	Kores et al. (2017)
T_{mean}, °C	Mean annual air temperature	8.0	11.0	Qin et al. (2018)
T_{ampl}, °C	Amplitude of air temperature	6.0	6.0	Kores et al. (2017)
Albedo, (–)	Albedo	0.20	0.21	Kores et al. (2017)
MCR, s m^{-1}	Minimum canopy resistance	131.0	121.0	Kores et al. (2017)

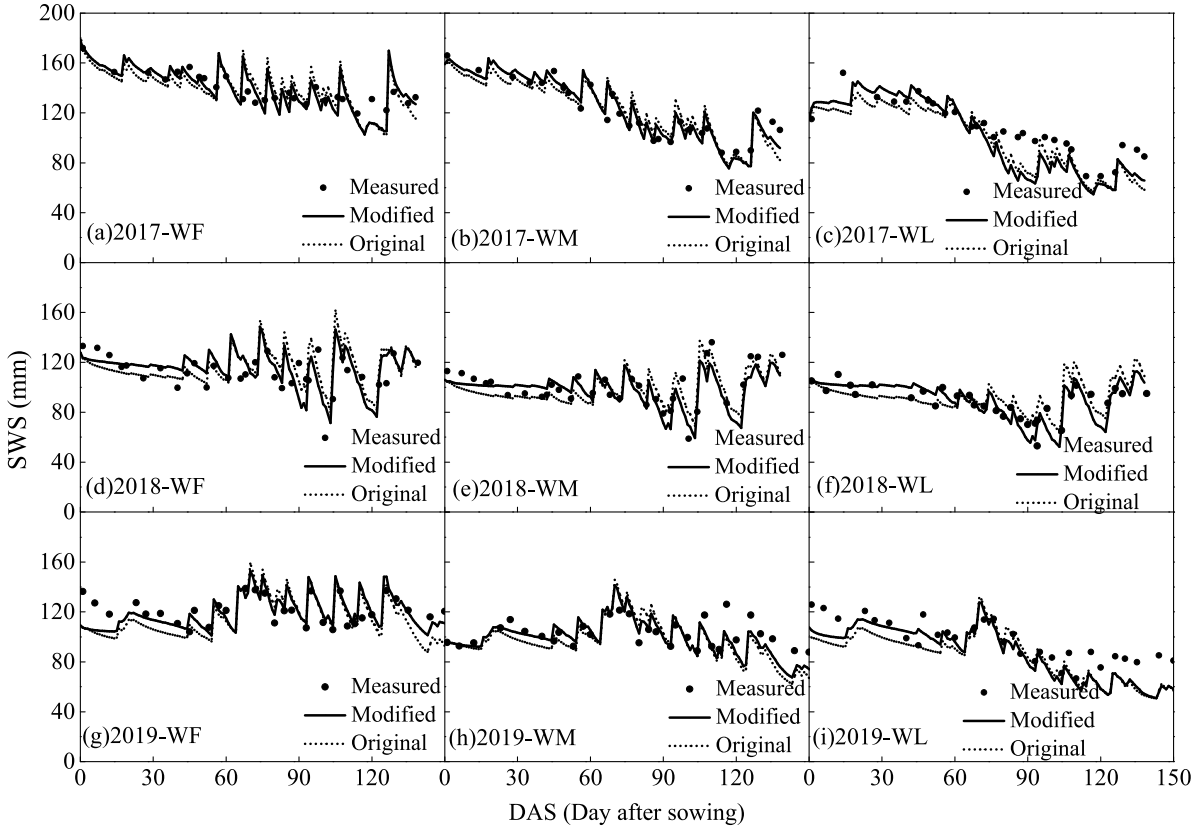

Fig. 2. Measured and simulated soil water storage (SWS) of 0–60 cm soil depths under WF, WM and WL treatments during the entire growing period in 2017 (a–c), 2018 (d–f) and 2019 (g–i).
Note: WF, full irrigation; WM, medium irrigation, 70%WF; WL, low irrigation, 40%WF.

Table 7
Model evaluation for SWS under WF, WM and WL treatments in 2017, 2018 and 2019.

Years	Treatments	Indices	Modified				Original			
			Early stage	Middle stage	Late stage	Total	Early stage	Middle stage	Late stage	Total
2017	WF	RMSE (mm)	4.30	13.47	12.56	11.00	7.49	14.33	14.56	12.54
		NRMSE (%)	2.87	10.17	9.76	8.02	5.00	10.82	11.32	9.14
		R^2	0.78	0.40	0.73	0.81	0.68	0.43	0.65	0.55
	WM	RMSE (mm)	3.86	10.16	10.22	8.91	6.21	11.73	14.25	10.65
		NRMSE (%)	2.70	9.25	10.00	7.52	4.34	10.69	13.95	8.99
		R^2	0.86	0.82	0.77	0.90	0.86	0.80	0.59	0.78
	WL	RMSE (mm)	9.07	23.03	14.54	17.27	11.85	17.74	17.22	15.32
		NRMSE (%)	6.93	22.39	17.83	16.19	9.05	17.25	21.12	14.36
		R^2	0.48	0.74	0.81	0.82	0.40	0.74	0.59	0.81
2018	WF	RMSE (mm)	7.48	16.79	11.99	15.99	8.15	22.52	15.18	16.85
		NRMSE (%)	6.48	15.19	10.52	14.49	7.06	21.61	13.32	15.27
		R^2	0.65	0.51	0.40	0.48	0.83	0.34	0.37	0.30
	WM	RMSE (mm)	7.26	6.64	15.57	9.52	10.17	8.02	10.61	9.46
		NRMSE (%)	7.20	7.26	13.16	9.44	10.08	8.77	8.97	9.38
		R^2	0.38	0.83	0.92	0.79	0.21	0.75	0.81	0.76
	WL	RMSE (mm)	5.91	8.97	8.80	8.10	8.41	7.64	11.70	9.01
		NRMSE (%)	6.05	11.24	9.26	9.10	8.62	9.58	12.31	10.12
		R^2	0.58	0.72	0.60	0.79	0.44	0.50	0.66	0.57
2019	WF	RMSE (mm)	13.45	5.79	6.96	9.42	16.15	7.83	13.07	12.81
		NRMSE (%)	11.25	4.73	5.73	7.78	13.51	6.39	10.76	10.57
		R^2	0.88	0.85	0.75	0.93	0.66	0.77	0.50	0.86
	WM	RMSE (mm)	5.26	5.47	15.05	9.52	6.49	8.28	18.95	12.26
		NRMSE (%)	5.21	5.21	14.78	9.28	6.42	7.89	18.61	11.94
		R^2	0.69	0.92	0.79	0.87	0.74	0.83	0.73	0.81
	WL	RMSE (mm)	12.74	8.17	19.53	13.86	17.98	6.59	19.73	15.59
		NRMSE (%)	11.45	8.62	24.09	14.34	16.16	6.95	24.33	16.13
		R^2	0.45	0.90	0.47	0.87	0.41	0.89	0.27	0.85

Note: RMSE, root mean square error; NRMSE, normalized root mean square error; R^2, coefficient of determination; Early stage, 0–60 DAS; Middle stage, 61–106 DAS; Late stage, after 107 DAS.

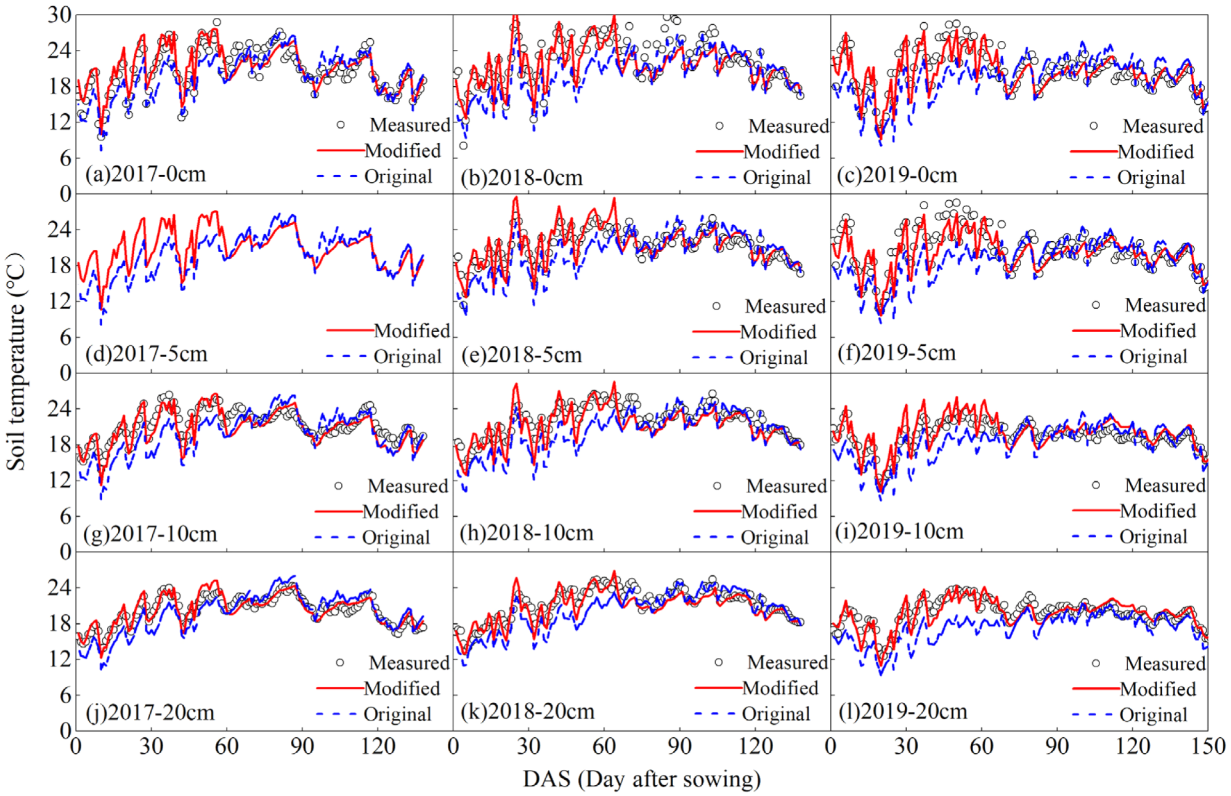

Fig. 3. Measured and simulated soil temperature at 0, 5, 10, 20 cm soil depths under WF treatment during the entire growing period in 2017 (a, d, g, j), 2018 (b, e, h, k) and 2019 (c, f, i, l).

percolation, surface runoff and lateral drainage. From the water balance component, soil water input through irrigation and precipitation was mainly consumed by evapotranspiration and deep percolation in this study (Table 11). Table 11 showed under drip irrigation, deep percolation only occurred under WF treatment. Previous studies showed that film mulching reduced evapotranspiration, which was mainly caused by the decrease of soil evaporation (Zhang et al., 2018b). Crop transpiration was an important component of evapotranspiration (Lopez–Olivari et al., 2016) and the vigorous growth of crops under film mulching led to the increase of crop transpiration (Yang et al., 2018). Through the comparison of the experimental results between the farmlands of film mulching and non–mulching, Zhang et al. (2018b) showed that the reduction rate of soil evaporation and evapotranspiration in mulched maize field were respectively 45.2% and 2.8%–5.2%, while the increase rate of crop transpiration was 5.9%–11.6% compared with the non–mulched conditions. Shen et al. (2019) concluded film mulching increased transpiration by 14.3% and decreased soil evaporation and evapotranspiration by 45.8% and 2.5% for maize. In our modified SWAP model, the reduction effect of soil evaporation was achieved by introducing the coefficient C_{film}, while the increase effect of crop transpiration were realized by the prosperous crop growth because of beneficial soil moisture/heat conditions as well as the advancement of crop development stage under film mulching. In summary, our simulations revealed that film mulching could decrease evapotranspiration. Furthermore, our modified model could also achieve the increase of evapotranspiration under film mulching conditions based on the bargaining between variations of evaporation and transpiration, able to explain such kind of conclusions drawn from previous studies (Chen et al., 2015; Xu et al., 2015).

Similar to its influence on evaporation and transpiration, film mulching could influence the SWS accordingly. It could cause the difference in the SWS between the modified and the original models. For example, at the early stage, soil evaporation was the main water loss due to the small canopy cover. The modified model showed the reduction of soil evaporation as well as the higher SWS than the original model. While at the middle stage, the SWS by the modified model was lower. It was because the modified model could show the more vigorous crop growth (Fig. 4) and stronger transpiration (Table 11). At the late stage, the SWS by the modified model could be similar (as in 2017 and 2018) or even a little higher (as in 2019) than that of the original model, because the advanced canopy senescence in the modified model (Fig. 4) could reduce the water consumption. Han et al. (2014) and Liang et al. (2017) had shown that the SWS in their modified model was higher than that of the original model in the whole growing period. It was because they assumed that film mulching greatly reduced soil evaporation, which could increase the SWS in the whole growing period. While in our modified model, we noticed the increased water consumption by transpiration which could reduce SWS at the middle stage. It demonstrated there were coupled effects between soil moisture/heat status and the crop water consumption/growth under film mulching conditions, which was captured in our modified model so that the stage changes of SWS under film mulching could be correctly revealed.

5.1.2. Soil temperature module evaluation

Soil temperature fluctuated with air temperature and was also affected by the surface cover, such as plastic film mulching (Li et al., 2013). The effect of plastic film mulching on soil temperature was related to the thermal and optical properties of plastic film under different climatic conditions (Bonachela et al., 2012; Liakatas et al., 1986; Zhang et al., 2017b). In this study, transparent plastic film was applied and generally the transparent plastic film mulching had heat preservation effect (Fan et al., 2016; Yang et al., 2018), which was also confirmed in our previous study (Zhao et al., 2018).

In this study, the effect of film mulching on soil temperature was considered by an empirical approach in the modified model and the

Table 8
Model evaluation for soil temperature at the soil depths of 0, 5, 10, 20 cm under WF, WM, WL treatments in 2017, 2018 and 2019.

Years	Soil layer (cm)	Indexes	Modified			Original		
			Early stage	Middle and late stages	Total	Early stage	Middle and late stages	Total
2017	0	RMSE (°C)	1.93	1.21	1.62	2.98	1.19	2.13
		NRMSE (%)	9.63	5.74	7.86	14.84	5.63	10.34
		R^2	0.94	0.99	0.85	0.91	0.99	0.78
	10	RMSE (°C)	1.45	1.45	1.60	3.87	1.51	2.73
		NRMSE (%)	6.88	6.76	7.52	18.31	7.05	12.85
		R^2	0.93	0.99	0.99	0.93	0.99	0.68
	20	RMSE (mm)	1.25	0.72	1.02	2.51	1.10	1.85
		RMSE (°C)	6.42	3.50	5.07	12.85	5.33	9.16
		R^2	0.93	0.99	0.88	0.93	0.99	0.77
2018	0	RMSE (°C)	1.76	2.15	1.90	4.30	1.88	3.06
		NRMSE (%)	8.15	9.47	8.54	19.87	8.29	13.77
		R^2	0.86	0.78	0.77	0.86	0.73	0.73
	5	RMSE (°C)	1.75	1.17	1.46	3.54	1.30	2.56
		NRMSE (%)	8.35	5.42	6.85	16.84	6.02	12.00
		R^2	0.91	0.73	0.81	0.91	0.75	0.64
	10	RMSE (°C)	1.98	1.53	1.74	4.13	1.49	2.85
		NRMSE (%)	9.22	6.78	7.91	19.25	6.63	12.93
		R^2	0.84	0.73	0.75	0.81	0.68	0.70
	20	RMSE (°C)	1.61	1.28	1.34	3.15	1.17	2.18
		NRMSE (%)	7.91	5.75	6.25	15.51	5.28	10.23
		R^2	0.86	0.75	0.79	0.85	0.69	0.76
2019	0	RMSE (°C)	1.80	1.29	1.53	4.80	1.83	3.42
		NRMSE (%)	8.33	6.51	7.41	22.25	9.22	16.61
		R^2	0.88	0.81	0.87	0.85	0.80	0.53
	5	RMSE (°C)	2.31	1.28	1.79	3.13	1.80	2.45
		NRMSE (%)	11.83	6.62	9.22	16.06	9.32	12.65
		R^2	0.85	0.73	0.77	0.83	0.73	0.63
	10	RMSE (°C)	2.00	1.18	1.58	3.36	1.50	2.47
		NRMSE (%)	10.30	6.11	8.16	17.30	7.73	12.71
		R^2	0.90	0.74	0.77	0.85	0.72	0.63
	20	RMSE (°C)	1.48	0.95	1.20	4.41	1.68	3.14
		NRMSE (%)	7.50	4.81	6.10	22.32	8.52	15.92
		R^2	0.85	0.77	0.81	0.84	0.74	0.60

results demonstrated that the simulated soil temperatures at 0, 5, 10, 20 cm soil depths during the entire growing period by the modified model were in better agreement with the measured values compared with the original model. Particularly, the regulating effect of plastic film on soil temperature was mainly reflected in the period when the canopy coverage was small, which led to the higher simulation accuracy for the soil temperature by the modified model than that of the original model at the early stage. Liang et al. (2017) concluded that RMSE of the soil temperature at 5 cm soil depth reduced from 4.22 °C to 1.13 °C, by 73.3% at the stage of LAI < 1 compared with the results of the original model. However, Han et al. (2014) reported that simulation accuracy was only improved by 16.0% at the early stage compared with the original model, which was smaller than our result (51.8%) and Liang et al. (2017). This may be because non–mulched surface temperature was set equal to the air temperature in Han et al. (2014), while it was estimated by the air temperature of the current day and previous day, as well as the soil surface temperature of the previous day in our study as shown in Eq. (1), which improved the model performance for soil temperature. With the continuous growth of crop canopy, the effect of film mulching on soil temperature decreased and crop canopy became the main factor to regulate the soil temperature (Flerchinger and Pierson, 1991). Therefore the simulated soil temperatures by both the modified and original models showed good fits with the measured values at the middle and late stages. In addition, for both the modified model and the original model, the highest simulation accuracy was found in the soil temperatures at 20 cm depth among the different soil layers (Table 8). This may be because the soil temperature at 20 cm depth was relatively stable and less disturbed by the external environment (Yang et al., 2019).

5.1.3. Crop growth and yield module evaluation

Crop growth had an influence on soil water and heat status by affecting the land surface energy distribution, partition of solar energy, and root zone development and water uptake, etc. (Liu et al., 2018). In turn, crop growth was also controlled by soil water and heat conditions and suitable soil water and heat conditions could promote crop growth (Dong et al., 2014). Our modified model showed that the film mulching increased the SWS and the soil temperature at the early stage, which was crucial for the crop development. In addition, the soil temperature at 5 cm soil depth was used to reflect the seed–maize growth in the modified model, which resulted in an increase of growing degree day (GDD) in the vegetative stage that directly related to leaf growth (Stone et al., 1999), inducing a more consistent LAI simulation result with the measured value at the early and middle stages. Our modified model showed a smaller LAI at the late stage than that of the original model. While Liang et al. (2017) reported that their modified model showed a higher LAI than that of the original model during the whole growing period. It was because our modified model considered the impact of soil temperature on crop development stage under film mulching conditions, which advanced the crop development stage. Therefore, when the crop canopy of modified model began to decline at the late stage, the crop canopy simulated by the original model was still in the vigorous period, which resulted in larger LAI. The similar effect of film mulching was revealed by previous experimental studies (Bu et al., 2013; Yang et al., 2018; Zhao et al., 2018), which compared the field data between film mulching and non–mulching. It demonstrated our modified model could more accurately evaluate the effect of film mulching on the LAI at different growth stages.

In general, the simulated LAI, ADB and yield by the modified model were more consistent with the measured values than that of the original model and the comparisons of RMSE of LAI, ADB, yield between the modified and original models also demonstrated the simulation accuracy of the modified model was greatly improved. Our modified model could be used for the evaluation of the LAI, ADB and yield of seed–-maize under film mulching conditions.

5.2. Evaluation of modified SWAP under different irrigation conditions

Our modified model performed well in the evaluation of the SWS, LAI, ADB and yield under the three irrigation cases. Film mulching in the modified model could reduce evaporation and increase the SWS at the early stage (Fig. 2), thus enhancing the LAI at the early and middle stages (Fig. 4) and the ADB and yield during the whole growing period (Fig. 5 and Table 11), which in turn reduced the SWS at the middle stage (Fig. 2). Results (Figs. 2, 4, 5 and Table 11) also indicated film mulching could influence SWS, LAI, ADB, yield, crop transpiration and WUE significantly especially under deficit irrigation. It demonstrated that film mulching played a crucial role under severe deficit irrigation (WL treatment), showing its potential advantage in arid area. A similar result based on field experiments was deduced by Yang et al. (2018), who suggested film mulching increased wheat yield and WUE by 11.8% and 16.7% under sufficient irrigation condition, while 16.6% and 27.6% under 50% sufficient irrigation condition compared with the non–mulching. Yu and Chai et al. (2015) indicated that film mulching improved the maize WUE by 6.1% and 29.3% under full irrigation level and 80% full irrigation level, respectively. The modified model could reflect the changes of the SWS, LAI, ADB, yield, water consumption and WUE caused by the film mulching under the various irrigation levels.

Soil evaporation was not influenced greatly by the irrigation conditions in both the modified and original models. It was because soil evaporation was relatively large only at the early stage, while there were only 2–3 times of irrigation and the irrigation amount was small at the early stage (Table 2), which led to the small difference of the SWS among different irrigation treatments. The more irrigation amounts, the more crop transpiration in both the modified and original models. It was related to the crop growth (Figs. 4 and 5) and the high LAI and ADB

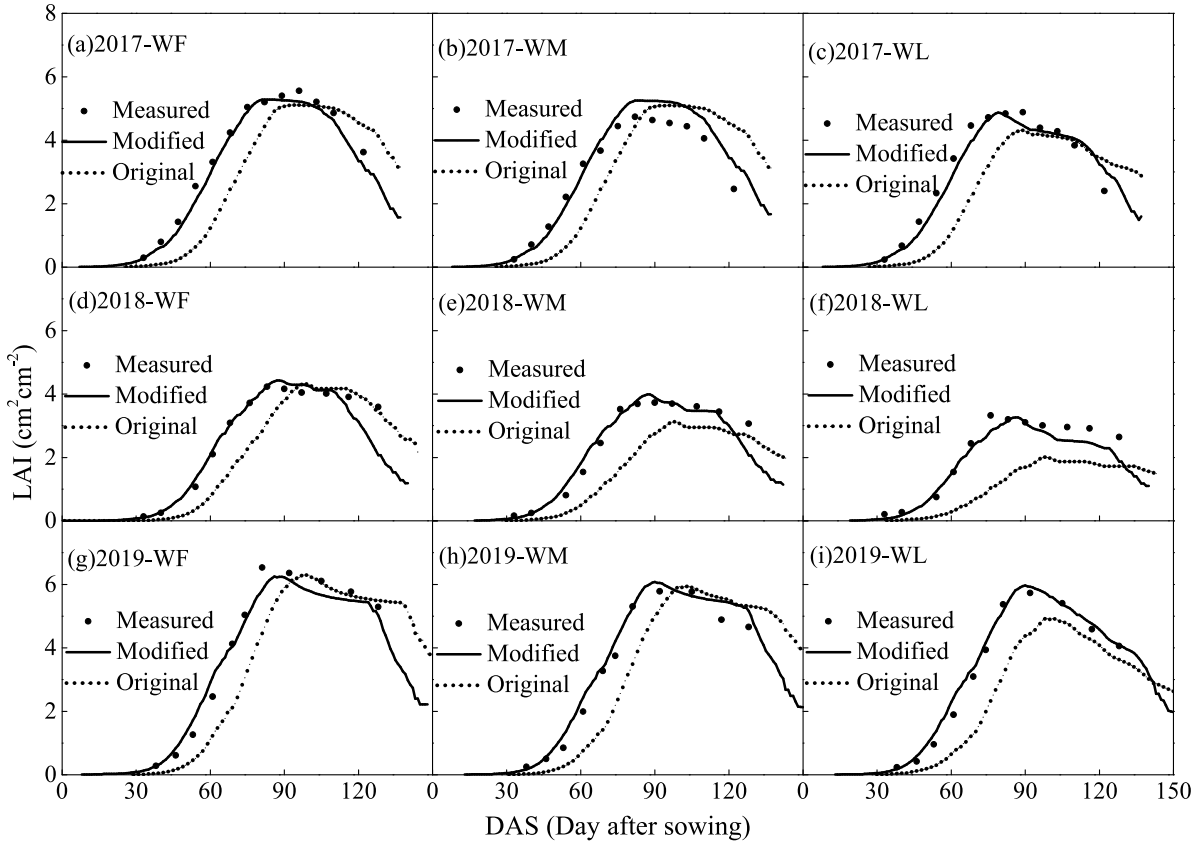

Fig. 4. Measured and simulated leaf area index (LAI) under WF, WM and WL treatments during the entire growing period in 2017 (a–c), 2018 (d–f) and 2019 (g–i).

Table 9
Model evaluation for LAI under WF, WM and WL treatments in 2017, 2018 and 2019.

Models	Treatments	Stages	2017			2018			2019		
			RMSE (cm^2cm^{-2})	NRMSE (%)	R^2	RMSE (cm^2cm^{-2})	NRMSE (%)	R^2	RMSE (cm^2cm^{-2})	NRMSE (%)	R^2
Modified	WF	Early and middle stages	0.23	6.39	0.99	0.14	5.60	0.99	0.39	11.75	0.98
		Late stage	0.34	8.04	0.99	0.80	20.88	0.99	0.22	3.91	0.99
		Total	0.25	6.78	0.99	0.42	14.65	0.98	0.37	9.19	0.99
	WM	Early and middle stages	0.41	13.21	0.99	0.18	8.02	0.99	0.20	7.55	0.99
		Late stage	0.74	22.62	0.99	0.50	14.80	0.95	0.60	12.57	0.90
		Total	0.48	15.19	0.98	0.29	11.73	0.98	0.32	9.39	0.99
	WL	Early and middle stages	0.29	9.03	0.99	0.24	11.91	0.98	0.22	8.00	0.99
		Late stage	0.52	16.56	0.99	0.51	17.98	0.93	0.17	3.83	0.99
		Total	0.34	10.45	0.96	0.33	14.89	0.96	0.21	6.41	0.99
Original	WF	Early and middle stages	1.21	33.99	0.91	1.01	39.70	0.89	1.39	41.66	0.91
		Late stage	0.61	14.32	0.97	0.19	4.84	0.95	0.16	2.93	0.96
		Total	1.13	31.05	0.86	0.88	30.64	0.86	1.26	31.56	0.90
	WM	Early and middle stages	1.02	32.90	0.92	1.14	51.51	0.91	1.23	45.35	0.93
		Late stage	1.56	47.83	0.98	0.52	15.39	0.94	0.69	14.35	0.95
		Total	1.12	35.83	0.86	1.02	40.74	0.85	1.15	34.18	0.90
	WL	Early and middle stages	1.29	39.74	0.88	1.42	71.35	0.83	1.42	52.46	0.94
		Late stage	0.70	22.58	0.99	1.02	36.05	0.93	0.36	8.22	0.99
		Total	1.22	37.76	0.84	1.33	60.45	0.80	1.29	39.83	0.90

under WF treatment consumed more water by transpiration than under WM and WL treatments. This resulted in the higher total crop evapotranspiration under WF treatment compared with that of the WM and WL treatments. DeJonge et al. (2012) concluded the maize evapotranspiration of the full irrigation was 8.7%–37.6% higher than that of the limit irrigation (no irrigation before the 12–leaf growth stage). Ran et al. (2017) considered the maize evapotranspiration under the irrigation of 70%–65% field capacity (FC) increased by 9.8%–16.2% and 27.0%–39.1% compared with that of the irrigation of 60%–55% FC and 50%–45% FC. Overall, our model could reflect the effect of different irrigation level on maize evapotranspiration.

5.3. Limitations of the modified SWAP and future work

The soil surface heat flow underneath the film is a complex process including energy balance and partition, heat conduction etc. under film mulching conditions (Ham and Kluitenberg, 1994; Liakatas et al., 1986). However, our current approach for the estimation of soil heat mainly focused on the empirical relationship with LAI and air temperature, as well as the film thickness and the thermal conductivity based on previous research, not considering the complex mechanism of plastic film mulching on the soil heat dynamics, which will be explored in our future work.

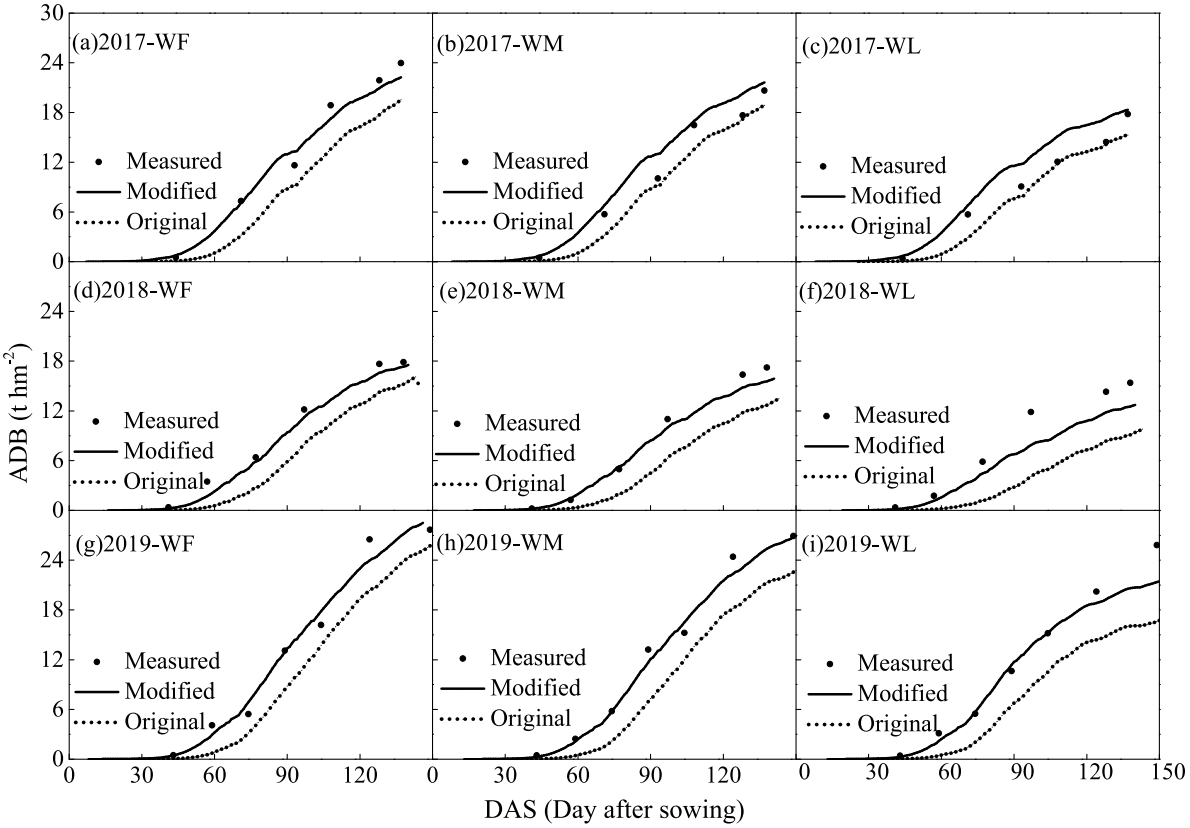

Fig. 5. Measured and simulated aboveground dry biomass (ADB) under WF, WM and WL treatments during the entire growing period in 2017 (a–c), 2018 (d–f) and 2019 (g–i).

In the modified SWAP, the root growth could be affected by the advancement of crop development stage caused by film mulching, while it had not been verified by specifically designed experiment yet. The precipitation interception ratio was also based on previous study that not verified specifically. Therefore, further field experiments should be designed and conducted to improve the result reliability.

In addition, the soil biological status was greatly influenced by the film mulching due to the change of redox state, soil temperature, soil moisture etc. However, this study focused on the soil water and heat conditions, with no limitation of nutrients on crop growth in our treatment. Therefore, the model needs to be further improved to consider the effect of film mulching on the soil biological status in the future work.

Despite these limitations, our modified model could adequately reflect the film mulching effect on soil water and heat conditions, as well as on the crop growth, water consumption, yield and WUE. It is especially useful because film mulching has been so widely used nowadays and concerns has raised regarding its potential impact on regional eco–hydrological process and even on climate change (Xu et al., 2011a; Zhang et al., 2017a). Supported by remote sensing, the modified SWAP, when embedded into regional hydrological model and general circulation model, could provide a powerful tool for evaluating the impacts of extensive use of film mulching.

6. Conclusions

The SWAP model algorithms in the module of precipitation interception, soil evaporation, soil temperature and crop growth stage were modified to accommodate the application of film mulching. The modified SWAP model performed better for the SWS, soil temperature, LAI, ADB and yield under different irrigation levels with film mulching than the original model. The staged changes of the SWS and LAI caused by the film mulching during the entire growing period could be reflected in modified model. The modified SWAP model demonstrated that film mulching could reduce the soil evaporation, increase the crop transpiration and improve the yield and WUE. Film mulching had more significant influence on the SWS, LAI, ADB, yield, crop transpiration and WUE under severe deficit irrigation (WL treatment) than under relatively high irrigation (WF and WM treatments). Note that the modified SWAP was calibrated based on our experimental field, which should be further verified in the other region and on various crops to improve the model applicability and reliability.

Table 10
Model evaluation for ADB under WF, WM and WL treatments in 2017, 2018 and 2019.

Models	Treatments	2017			2018			2019		
		R^2	RMSE (t hm^{-2})	NRMSE (%)	R^2	RMSE (t hm^{-2})	NRMSE (%)	R^2	RMSE (t hm^{-2})	NRMSE (%)
Modified	WF	0.99	1.25	8.88	0.99	1.12	11.60	0.98	1.39	10.43
	WM	0.98	1.74	14.69	1.00	1.32	15.47	0.99	1.22	9.65
	WL	0.81	2.10	21.17	0.98	2.29	27.81	0.98	1.87	16.19
Original	WF	0.98	3.83	27.28	0.96	3.53	36.54	0.97	3.73	27.90
	WM	0.98	1.77	14.98	0.97	2.77	32.61	0.98	4.43	35.07
	WL	0.97	1.62	16.34	0.91	3.76	45.56	0.98	4.56	39.49

Table 11
The simulated water budgets, yield and water use efficiency (WUE) under WF, WM and WL treatments in 2017, 2018 and 2019.

Years	Treatments	Water balance components (mm)								Yield (t hm^{-2})			WUE (kg m^{-3})
		P	ΔP	I	T	E	ET	D	ΔW	Measured	Simulated	NRMSE (%)	
2017	WF–Modified	133.8	38.9	306.4	330.2	60.4	390.6	30.2	19.5	7.19	7.34	2.09	1.88
	WF–Original	133.8	14.6	306.4	281.1	157.9	439.0	23.5	36.9		5.30	26.29	1.21
	WM–Modified	133.8	38.6	214.5	323.3	60.9	384.2	0.0	74.5	6.83	6.77	0.88	1.76
	WM–Original	133.8	14.6	214.5	268.1	155.4	423.5	0.0	89.8		5.07	25.77	1.20
	WL–Modified	133.8	37.4	122.6	248.1	59.9	308.0	0.0	89.0	5.68	5.21	8.27	1.69
	WL–Original	133.8	12.4	122.6	194.8	151.1	345.9	0.0	101.9		3.50	38.42	1.01
2018	WF–Modified	178.4	50.1	279.0	378.6	55.0	433.6	4.8	31.1	5.14	5.34	3.82	1.23
	WF–Original	178.4	15.9	279.0	353.1	137.3	490.4	3.6	52.5		4.38	14.84	0.89
	WM–Modified	178.4	49.8	195.3	303.4	56.0	359.4	0.0	35.5	4.94	4.90	0.86	1.36
	WM–Original	178.4	12.2	195.3	253.8	144.1	397.9	0.0	36.4		3.92	20.67	0.99
	WL–Modified	178.4	48.2	111.6	234.8	59.4	294.2	0.0	52.4	3.91	4.09	4.60	1.39
	WL–Original	178.4	7.9	111.6	173.4	145.8	319.2	0.0	37.1		2.96	24.25	0.93
2019	WF–Modified	156.8	44.9	288.8	337.9	52.6	390.5	1.7	–8.5	9.25	9.01	2.59	2.31
	WF–Original	156.8	18.4	288.8	309.1	136.4	445.5	1.2	19.5		7.05	23.76	1.58
	WM–Modified	156.8	46.0	202.2	300.7	51.2	351.9	0.0	38.9	7.46	8.30	11.26	2.36
	WM–Original	156.8	16.7	202.2	257.0	134.2	391.2	0.0	48.9		5.40	27.61	1.38
	WL–Modified	156.8	45.0	115.5	244.5	55.2	299.7	0.0	72.4	5.78	5.04	12.80	1.68
	WL–Original	156.8	13.4	115.5	188.4	137.0	325.4	0.0	66.5		3.08	46.71	0.95

Note: P, precipitation; ΔP, precipitation interception (canopy and film interception); I, total irrigation; T, transpiration; E, evaporation; ET, evapotranspiration; D, deep percolation; ΔW, change of SWS between planting and harvesting period; WUE = Yield/ET.

Declaration of Competing Interest

The authors declare that they have no known competing financial interests or personal relationships that could have appeared to influence the work reported in this paper.

Acknowledgments

This work was supported by the National Natural Science Foundation of China (51679234, 51790535). Authors thank New Mexico Agricultural Experiment Station for support and Frank Sholedice for editorial assistance.

References

Alliaume, F., Rossing, W.A.H., Tittonell, P., Dogliotti, S., 2016. Modelling soil tillage and mulching effects on soil water dynamics in raised–bed vegetable rotations. Eur. J. Agron. 82, 268–281. https://doi.org/10.1016/j.eja.2016.08.011.

Anikwe, M.A.N., Mbah, C.N., Ezeaku, P.I., Onyia, V.N., 2007. Tillage and plastic mulch effects on soil properties and growth and yield of cocoyam (Colocasia esculenta) on an ultisol in southeastern Nigeria. Soil Tillage Res. 93, 264–272. https://doi.org/10.1016/j.still.2006.04.007.

Balashov, E., Buchkina, N., Rizhiya, E., Farkas, C., 2014. Field validation of DNDC and SWAP models for temperature and water content of loamy and sandy loam Spodosols. Int. Agrophys. 28, 133–142. https://doi.org/10.2478/intag-2014-0001.

Bonachela, S., Granados, M.R., López, J.C., Hernández, J., Magán, J.J., Baeza, E.J., Baille, A., 2012. How plastic mulches affect the thermal and radiative microclimate in an unheated low–cost greenhouse. Agric. For. Meteorol. 152, 65–72. https://doi.org/10.1016/j.agrformet.2011.09.006.

Boogaard, H.L., Diepen, V., C.A., Roetter, R.P., Cabrera, J.M.C.A., Laar, van, H.H., 1998. User's Guide For The WOFOST 7.1 Crop Growth Simulation Model and WOFOST Control Center 1.5. Technical Document/DLO–Winand Staring Centre 52.

Braden, H., 1985. Ein Energiehaushalts–und verdunstungsmodell for wasser und stoff-haushaltsuntersuchungen landwirtschaftlich genutzer einzugsgebiete. Mittelungen Dtsch. Bodenkd. Geselschaft 42, 294–299.

Bu, L.D., Liu, J.L., Zhu, L., Luo, S.S., Chen, X.P., Li, S.Q., Hill, R.L., Zhao, Y., 2013. The effects of mulching on maize growth, yield and water use in a semi–arid region. Agric. Water Manag. 123, 71–78. https://doi.org/10.1016/j.agwat.2013.03.015.

Chakraborty, D., Garg, R.N., Tomar, R.K., Singh, R., Sharma, S.K., Singh, R.K., Trivedi, S.M., Mittal, R.B., Sharma, P.K., Kamble, K.H., 2010. Synthetic and organic mulching and nitrogen effect on winter wheat (Triticum aestivum L.) in a semi–arid environment. Agric. Water Manag. 97, 738–748. https://doi.org/10.1016/j.agwat.2010.01.006.

Chen, Y.L., Liu, T., Tian, X.H., Wang, X.F., Li, M., Wang, S.X., Wang, Z.H., 2015. Effects of plastic film combined with straw mulch on grain yield and water use efficiency of winter wheat in Loess Plateau. Field Crops Res. 172, 53–58. https://doi.org/10.1016/j.fcr.2014.11.016.

Cheng, Z.Q., Meng, J.H., Wang, Y.M., 2016. Improving spring maize yield estimation at field scale by assimilating time–series HJ–1 CCD data into the WOFOST model using a new method with fast algorithms. Remote Sens. 8, 303. https://doi.org/10.3390/rs8040303.

Crescimanno, G., Morga, F., Ventrella, D., 2012. Application of the SWAP model to predict impact of climate change on soil water balance in a Sicilian vineyard. Ital. J. Agron. 7, e17. https://doi.org/10.4081/ija.2012.e17.

Dong, B.D., Liu, M.Y., Jiang, J.W., Shi, C.H., Wang, X.M., Qiao, Y.Z., Liu, Y.Y., Zhao, Z.H., Li, D.X., Si, F.Y., 2014. Growth, grain yield, and water use efficiency of rain–fed spring hybrid millet (Setaria italica) in plastic–mulched and un mulched fields. Agric. Water Manag. 143, 93–101. https://doi.org/10.1016/j.agwat.2014.06.011.

Du, T.S., Kang, S.Z., Hu, X.T., Yang, X.Y., 2005. Effect of alternate partial root–zone drip irrigation on yield and water use efficiency of cotton. Sci. Agric. Sin. 38 (10), 2061–2068. https://doi.org/10.3321/j.issn:0578-1752.2005.10.017. (in Chinese with English abstract).

Dejonge, K.C., Ascough II, J.C., Andales, A.A., Hansen, N.C., Garcia, L.A., Arabi, M., 2012. Improving evapotranspiration simulations in the CERES–Maize model under limited irrigation. Agric. Water Manag. 115, 92–103. https://doi.org/10.1016/j.agwat.2012.08.013.

Fan, Y.L., Zhang, W.N., Kang, Y.C., Zhao, Z.P., Yao, K., Qin, S.H., 2019. Effects of ridge and furrow film mulching on soil environment and yield under potato continuous cropping system. Plant Soil Environ. 65, 523–529. https://doi.org/10.17221/481/2019-PSE.

Fan, Y.Q., Ding, R.S., Kang, S.Z., Hao, X.M., Du, T.S., Tong, L., Li, S.E., 2016. Plastic mulch decreases available energy and evapotranspiration and improves yield and water use efficiency in an irrigated maize cropland. Agric. Water Manag. 179, 122–131. https://doi.org/10.1016/j.agwat.2016.08.019.

Feddes, R.A., Kowalik, P.J., Zaradny, H., 1978. Simulation of Field Water Use and Crop Yield. Pudoc, Wageningen, Netherlands.

Flerchinger, G.N., Pierson, F.B., 1991. Modeling plant canopy effects on variability of soil temperature and water. Agric. For. Meteorol. 56 (3), 227–246. https://doi.org/10.1016/0168-1923(91)90093-6.

Ham, J.M., Kluitenberg, G.J., 1994. Modeling the effect of mulch optical properties and mulch–soil contact resistance on soil heating under plastic mulch culture. Agric. For. Meteorol. 71, 403–424. https://doi.org/10.1016/0168-1923(94)90022-1.

Han, J., Jia, Z.K., Wu, W., Li, C.S., Han, Q.F., Zhang, J., 2014. Modeling impacts of film mulching on rainfed crop yield in Northern China with DNDC. Field Crops Res. 155, 202–212. https://doi.org/10.1016/j.fcr.2013.09.004.

Haraguchi, T., Marui, A., Mori, K., Nakano, Y., 2003. Movement of water collected by vegetables in plastic–mulching field. J. Fac. Agric. Kyushu Univ. 48 (1-2), 237–245.

He, Q.S., Li, S.E., Kang, S.Z., Yang, H.B., Qin, S.J., 2018. Simulation of water balance in a maize field under film–mulching drip irrigation. Agric. Water Manag. 210, 252–260. https://doi.org/10.1016/j.agwat.2018.08.005.

Hou, P., Cui, Z.L., Bu, L.D., Yang, H.S., Zhang, F.S., Li, S.K., 2014. Evaluation of a modified hybrid–Maize model incorporating a newly developed module of plastic film mulching. Crop Sci. 54 (6), 2796–2804. https://doi.org/10.2135/cropsci2013.11.0747.

Hornung, U., Messing, W., 1983. Truncation errors in the numerical solution of horizontal diffusion in saturated/unsaturated media. Adv. Water Resour. 6 (3), 165–168. https://doi.org/10.1016/0309-1708(83)90029-5.

Huang, J.X., Ma, H.Y., Su, W., Zhang, X.D., Huang, Y.B., Fan, J.L., Wu, W.B., 2015. Jointly assimilating MODIS LAI and ET products into the SWAP model for winter wheat yield estimation. IEEE J. Sel. Top. Appl. Earth Obs. Remote Sens. 8 (8), 4060–4071. https://doi.org/10.1109/JSTARS.2015.2403135.

Jamieson, P.D., Porter, J.R., Wilson, D.R., 1991. A test of the computer simulation model ARCWHEAT1 on wheat crops grown in New Zealand. Field Crop Res. 27, 337–350. https://doi.org/10.1016/0378-4290(91)90040-3.

Jiang, J., Feng, S.Y., Huo, Z.L., Zhao, Z.C., Jia, B., 2011. Application of the SWAP model to simulate water–salt transport under deficit irrigation with saline water. Math.

Comput. Model. 54, 902–911. https://doi.org/10.1016/j.mcm.2010.11.014.
Jones, C.A., Kiniry, J.R., 1986. CERES–maize: a simulation model of maize growth and development. Agric. For. Meteorol. 41 (3), 339. https://doi.org/10.1016/0168-1923(87)90089-X. 339.
Karthe, D., Chalov, S., Borchardt, D., 2014. Water resources and their management in central Asia in the early twenty first century: status, challenges and future prospects. Environ. Earth Sci. 73, 487–499. https://doi.org/10.1007/s12665-014-3789-1.
Kamyab–Talesh, F., Mostafazadeh–Fard, B., Vazifedoust, M., Shayannejad, M., Navabian, M., 2017. Salt tolerance analysis of crops using the SWAP model. Biosci. Biotechnol. Res. Asia 14, 643–649. https://doi.org/10.13005/bbra/2490.
Kim, Y.S., Sina, B., Janine, F.K., John, T., Edwin, H., Kiese, R., 2014. Simulation of N_2O emissions and nitrate leaching from plastic mulch radish cultivation with LandscapeDNDC. Ecol. Res. 29 (3), 441–454. https://doi.org/10.1007/s11284-014-1136-3.
Kroes, J.G., Wesseling, J.G., Van Dam, J.C., 2000. Integrated modelling of the soil–water–atmosphere–plant system using the model SWAP 2.0, an overview of theory and an application. Hydrol. Process. 14, 1993–2002. https://doi.org/10.1002/1099-1085(20000815/30)14:11/123.0.CO;2-#.
Kroes, J.G., Dam, J.C.V., Barthoiomeus, R.P., Groenendijk, P., Heinen, M., Hendriks, R.F.A., Mulder, H.M., Supit, I., Walsum, P.E.V., 2017. SWAP Version 4: Theory Description and User Manual. Wageningen Environmental Research, Wageningen, Netherlands.
Kumar, P., Sarangi, A., Singh, D.K., Parihar, S.S., Sahoo, R.N., 2015. Simulation of salt dynamics in the root zone and yield of wheat crop under irrigated saline regimes using SWAP model. Agric. Water Manag. 148, 72–83. https://doi.org/10.1016/j.agwat.2014.09.014.
Li, J., Jiao, X.Y., Jiang, H.Z., Song, J., Chen, L.N., 2020. Optimization of irrigation scheduling for maize in an arid oasis based on simulation–optimization model. Agron. J. 10, 935. https://doi.org/10.3390/agronomy10070935.
Li, R., Hou, X.Q., Jia, Z.K., Han, Q.F., Ren, X.L., Yang, B.P., 2013. Effects on soil temperature, moisture, and maize yield of cultivation with ridge and furrow mulching in the rainfed area of the Loess Plateau, China. Agric. Water Manag 116, 101–109. https://doi.org/10.1016/j.agwat.2012.10.001.
Li, Y., 2002. Experimental Studies on the Coupled Movement of Soil Water, Salt, and Heat Transfer Under Plastic Mulch. Xi'an University of Technology (in Chinese with English abstract).
Liang, H., Hu, K.L., Qin, W., Zuo, Q., Zhang, Y.N., 2017. Modelling the effect of mulching on soil heat transfer, water movement and crop growth for ground cover rice production system. Field Crops Res. 201, 97–107. https://doi.org/10.1016/j.fcr.2016.11.003.
Liakatas, A., Clark, J.A., Monteith, J.L., 1986. Measurements of the heat balance under plastic mulches. Part I. Radiation balance and soil heat flux. Agric. For. Meteorol. 36, 227–239. https://doi.org/10.1016/0168-1923(86)90037-7.
Liu, B., Yang, L., Zeng, Y.D., Yang, F., Yang, Y.Z., Lu, Y.H., 2018. Secondary crops and non–crop habitats within landscapes enhance the abundance and diversity of generalist predators. Agric. Ecosyst. Environ. 258, 30–39. https://doi.org/10.1016/j.agee.2018.02.007.
Liu, L., Guo, Z.Z., Huang, G.H., Wang, R.T., 2019. Water productivity evaluation under multi-GCM projections of climate change in Oases of the Heihe River Basin, Northwest China. Inter. J. Environ. Res. Public Health 16, 1706. https://doi.org/10.3390/ijerph16101706.
Lopez–Olivari, R., Ortega–Farías, S., Poblete–Echeverría, C., 2016. Partitioning of net radiation and evapotranspiration over a super intensive drip–irrigated olive orchard. Irrig. Sci. 34 (1), 17–31. https://doi.org/10.1007/s00271-015-0484-2.
Ma, G.N., Huang, J.X., Wu, W.B., Fan, J.L., Zou, J.Q., Wu, S.J., 2013. Assimilation of MODIS–LAI into the WOFOST model for forecasting regional winter wheat yield. Math. Comput. Model. 58, 634–643. https://doi.org/10.1016/j.mcm.2011.10.038.
Ma, W.W., Jin, X.X., Shi, J.C., Ning, S.R., Li, S., Tao, Y.Y., Zhang, Y.N., Zuo, Q., 2015. Modeling increasing effect of soil temperature through plastic film mulch in ground cover rice production system using CERES–Rice. Trans. CSAE 31 (9), 215–222. https://doi.org/10.11975/j.issn.1002-6819.2015.09.033. (in Chinese with English abstract).
Ma, W.W., Shi, J.C., Jin, X.X., Ning, S.R., Li, S., Tao, Y.Y., Zhang, Y.N., Liu, Y., Lin, S., Hu, P.C., Zuo, Q., 2017. Rice growth simulation under film mulching in dryland through improving CERES–Rice model. Trans. CSAE 33 (6), 115–123. https://doi.org/10.11975/j.issn.1002-6819.2017.06.015. (in Chinese with English abstract).
Martínez-Ferri, E., Muriel-Fernández, J.L., Díaz, J.A.Rodríguez, 2013. Soil water balance modelling using SWAP: an application for irrigation water management and climate change adaptation in citrus. Outlook Agric. 42 (2), 93–102. https://doi.org/10.5367/oa.2013.0125.
Maurya, P.R., Lal, R., 1981. Effects of different mulch materials on soil properties and on the root growth and yield of maize (Zea mays) and cowpea (Vigna unguiculata). Field Crop Res. 4, 33–45. https://doi.org/10.1016/0378-4290(81)90052-6.
Mokhtari, A., Noory, H., Vazifedoust, M., 2018. Improving crop yield estimation by assimilating LAI and inputting satellite-based surface incoming solar radiation into SWAP model. Agric. For. Meteorol. 250, 159–170. https://doi.org/10.1016/j.agrformet.2017.12.250.
Qin, S.J., Li, S.E., Yang, K., Hu, K.L., 2018. Can plastic mulch save water at night in irrigated croplands? J. Hydrol. 564, 667–681. https://doi.org/10.1016/j.jhydrol.2018.07.050.
Ramakrishna, A., Tam, H.M., Wani, S.P., Long, T.D., 2006. Effect of mulch on soil temperature, moisture, weed infestation and yield of groundnut in northern Vietnam. Field Crop Res. 95 (2–3), 115–125. https://doi.org/10.1016/j.fcr.2005.01.030.
Ran, H., Kang, S.Z., Li, F.S., Du, T.S., Ding, R.S., Li, S.E., 2017. Responses of water productivity to irrigation and N supply for hybrid maize seed production in an arid region of Northwest China. J. Arid Land 9 (4), 504–514. https://doi.org/10.1007/s40333-017-0017-3.
Ren, X.L., Jia, Z.K., Chen, X.L., 2008. Rainfall concentration for increasing corn production under semiarid climate. Agric. Water Manag. 95 (12), 1293–1302. https://doi.org/10.1016/j.agwat.2008.05.007.
Ren, X.L., Chen, X.L., Cai, T., Wei, T., Wu, Y., Ali, S., Zhang, P., Jia, Z.K., 2017. Effects of ridge–furrow system combined with different degradable mulching materials on soil water conservation and crop production in semi–humid areas of China. Front. Plant Sci. 8, 1877. https://doi.org/10.3389/fpls.2017.01877.
Richards, L.A., 1931. Capillary conduction of liquids through porous mediums. Phys. College Park Md 1 (5), 318–333. https://doi.org/10.1063/1.1745010.
Shen, Q.X., Ding, R.S., Du, T.S., Tong, L., Li, S.E., 2019. Water use effectiveness is enhanced using film mulch through increasing transpiration and decreasing evapotranspiration. Water Basel 11, 1153. https://doi.org/10.3390/w11061153.
Šimůnek, J., Šejna, M., van Genuchten, M.Th., 1999. The Hydrus–2D Software Package for Simulating Two–Dimensional Movement of Water, Heat and Multiple Solutes in Variably Saturated Media. Version 2.0, IGWMC–TPS–53. International Groundwater Modeling Center, Colorado School of Mines, Golden, CO, USA.
Stone, P.J., Sorensen, I.B., Jamieson, P.D., 1999. Effect of soil temperature on phenology, canopy development, biomass and yield of maize in a cool–temperate climate. Field Crop Res. 63 (2), 169–178. https://doi.org/10.1016/S0378-4290(99)00033-7.
Van Dam, J.C., Groenendijk, P., Hendriks, R.F.A., Kroes, J.G., 2008. Advances of modeling water flow in variably saturated soils with SWAP. Vadose Zone J. 7, 640. https://doi.org/10.2136/vzj2007.0060.
Van Genuchten, M.T., 1980. A closed–form equation for predicting the hydraulic conductivity of unsaturated soils. Soil Sci. Soc. Am. J. 44, 892–898. https://doi.org/10.2136/sssaj1980.03615995004400050002x.
Wilkerson, G.G., Jones, J.W., Boote, K.J., Ingram, K.T., Mishoe, J.W., 1983. Modeling soybean growth for crop management. Trans. ASAE 26, 63–73. https://doi.org/10.13031/2013.33877.
Wu, Y.J., Du, T.S., Ding, R., Yuan, Y.S., Li, S.E., Tong, L., 2017. An isotope method to quantify soil evaporation and evaluate water vapor movement under plastic film mulch. Agric. Water Manag. 184, 59–66. https://doi.org/10.1016/j.agwat.2017.01.005.
Xu, J., Li, C.F., Liu, H.T., Zhou, P.L., Tao, Z.Q., Wang, P., Meng, Q.F., Zhao, M., 2015. The effects of plastic film mulching on maize growth and water use in dry and rainy years in Northeast China. PLoS ONE 10 (5), e0125781. https://doi.org/10.1371/journal.pone.0125781.
Xu, X., Huang, G.H., Qu, Z.Y., Huang, Q.Z., 2011a. Regional scale model for simulating soil water flow and solute transport processes–GSWAP. Trans. CSAE 27 (7), 58–63. https://doi.org/10.3969/j.issn.1002-6819.2011.07.010.
Xu, X., Huang, G.H., Zhan, H.B., Qu, Z.Y., Huang, Q.Z., 2011b. Integration of SWAP and MODFLOW-2000 for modeling groundwater dynamics in shallow water table areas. J. Hydrol. 412, 170–181. https://doi.org/10.1016/j.jhydrol.2011.07.002.
Yang, J., Mao, X.M., Wang, K., Yang, W.C., 2018. The coupled impact of plastic film mulching and deficit irrigation on soil water/heat transfer and water use efficiency of spring wheat in Northwest China. Agric. Water Manag. 201, 232–245. https://doi.org/10.1016/j.agwat.2017.12.030.
Yang, N., Sun, Z.X., Zhang, L.Z., Zheng, J.M., Feng, L.S., Li, K.Y., Zhang, Z., Feng, C., 2015. Simulation of water use process by film mulched cultivated maize based on improved AquaCrop model and its verification. Trans. CSAE 31, 122–132. https://doi.org/10.3969/j.issn.1002-6819.2015.z1.015.
Yang, W.C., Mao, X.M., Yang, J., Ji, M.M., Adeloye, A.J., 2019. A coupled model for simulating water and heat transfer in soil–plant–atmosphere continuum with crop growth. Water Basel 11, 47. https://doi.org/10.3390/w11010047.
Yu, A.Z., Chai, Q., 2015. Effects of plastic film mulching and irrigation quota on yield of corn in arid oasis irrigation area. Acta Agron. Sin. 41, 778–786. https://doi.org/10.3724/SP.J.1006.2015.00778.
Yuan, C.F., Feng, S.Y., Huo, Z.L., Ji, Q.Y., 2019. Simulation of Saline Water Irrigation for Seed Maize in Arid Northwest China Based on SWAP Model. Sustainability 11, 4264. https://doi.org/10.3390/su11164264.
Zhang, Y., Li, C.S., Trettin, C.C., Li, H., Sun, G., 2002. An integrated model of soil, hydrology, and vegetation for carbon dynamics in wetland ecosystems. Global Biogeochem. Cycles 16 (4), 1061–1077. https://doi.org/10.1029/2001GB001838.
Zhang, Y., Zhao, Y., Wang, C., Chen, S.N., 2017a. Using statistical model to simulate the impact of climate change on maize yield with climate and crop uncertainties. Theor. Appl. Climatol. 130, 1065–1071. https://doi.org/10.1007/s00704-016-1935-2.
Zhang, Y.L., Wang, F.X., Shock, C.C., Yang, K.J., Kang, S.Z., Qin, J.T., Li, S.E., 2017b. Effects of plastic mulch on the radiative and thermal conditions and potato growth under drip irrigation in arid Northwest China. Soil Tillage Res. 172, 1–11. https://doi.org/10.1016/j.still.2017.04.010.
Zhang, Y.Q., Wang, J.D., Gong, S.H., Xu, D., Sui, J., Wu, Z.D., Mo, Y., 2018. Effects of film mulching on evapotranspiration, yield and water use efficiency o f a maize field with drip irrigation in Northeastern China. Agric. Water Manag. 205, 90–99. https://doi.org/10.1016/j.agwat.2018.04.029.
Zhang, Y.Y., Han, H.K., Zhang, D.Z., Li, J., Gong, X.W., Feng, B.L., Xue, Z.H., Yang, P., 2017c. Effects of ridging and mulching combined practices on proso millet growth and yield in semi–arid regions of China. Field Crops Res. 213, 65–74. https://doi.org/10.1016/j.fcr.2017.06.015.
Zheng, D., Hunt, E.R., Running, S.W., 1993. A daily soil temperature model based on air temperature and precipitation for continental applications. Clim. Res. 2, 183–191. https://doi.org/10.3354/cr002183.
Zhao, Y., Mao, X.M., Duan, M., 2018. Effects of film mulching and irrigation amount on farmland water–heat dynamics and growth of seed–maize. Trans. CSAM 49 (8), 275–284. https://doi.org/10.6041/j.issn.1000-1298.2018.08.032. (in Chinese with English abstract).